Moho and basement depth in the NE Atlantic Ocean based on seismic refraction data and receiver functions

THOMAS FUNCK[1]*, WOLFRAM H. GEISSLER[2], GEOFFREY S. KIMBELL[3], SOFIE GRADMANN[4], ÖGMUNDUR ERLENDSSON[5], KENNETH McDERMOTT[6] & UNI K. PETERSEN[7]

[1]*Geological Survey of Denmark and Greenland, Øster Voldgade 10, 1350 Copenhagen K, Denmark*

[2]*Alfred Wegener Institute Helmholtz Centre for Polar and Marine Research, Am Alten Hafen 26, 27568 Bremerhaven, Germany*

[3]*British Geological Survey, Keyworth, Nottingham NG12 5GG, UK*

[4]*Geological Survey of Norway, Leiv Eirikssons vei 39, 7040 Trondheim, Norway*

[5]*Iceland Geosurvey, Grensásvegi 9, 108 Reykjavík, Iceland*

[6]*UCD School of Geological Sciences, University College Dublin, Belfield, Dublin 4, Ireland*

[7]*Faroese Earth and Energy Directorate, Brekkutún 1, 110 Tórshavn, Faroe Islands*

**Correspondence: tf@geus.dk*

Abstract: Seismic refraction data and results from receiver functions were used to compile the depth to the basement and Moho in the NE Atlantic Ocean. For interpolation between the unevenly spaced data points, the kriging technique was used. Free-air gravity data were used as constraints in the kriging process for the basement. That way, structures with little or no seismic coverage are still presented on the basement map, in particular the basins off East Greenland. The rift basins off NW Europe are mapped as a continuous zone with basement depths of between 5 and 15 km. Maximum basement depths off NE Greenland are 8 km, but these are probably underestimated. Plate reconstructions for Chron C24 (*c.* 54 Ma) suggest that the poorly known Ammassalik Basin off SE Greenland may correlate with the northern termination of the Hatton Basin at the conjugate margin. The most prominent feature on the Moho map is the Greenland–Iceland–Faroe Ridge, with Moho depths >28 km. Crustal thickness is compiled from the Moho and basement depths. The oceanic crust displays an increased thickness close to the volcanic margins affected by the Iceland plume.

The rifting in the NE Atlantic Ocean region (Fig. 1) occurred in several episodes spanning from the Carboniferous Period to the early Cenozoic break-up (e.g. Ziegler 1988; Doré *et al.* 1999). Seafloor spreading propagated from the Central Atlantic Ocean northwards into the NE Atlantic Ocean (Srivastava & Tapscott 1986), where spreading between Greenland and NW Europe began in the Early Eocene (Storey *et al.* 2007). Large sections of the continental margins fringing the NE Atlantic Ocean are magma-rich margins with extensive flood-basalt volcanism and igneous intrusions (e.g. Eldholm & Grue 1994; Holbrook *et al.* 2001). The amount of break-up-related magmatism depends on the distance to the Iceland plume (Holbrook *et al.* 2001). Furthermore, the plume has profoundly influenced the creation of oceanic crust throughout the NE Atlantic region (Howell *et al.* 2014). The influence of the plume appears to extend further to the south along the Reykjanes Ridge than to the north along the Kolbeinsey Ridge (Hooft *et al.* 2006). The most outstanding feature on the bathymetric map is the Greenland–Iceland–Faroe Ridge (composed of the Greenland–Iceland Ridge, Iceland and the Iceland–Faroe Ridge: Fig. 1), the result of enhanced melting in the Iceland plume (White & McKenzie 1995; Staples *et al.* 1997). Most of the NE Atlantic Ocean has shallower bathymetry and hotter mantle when compared to other oceans (Parkin & White 2008; Artemieva & Thybo 2013).

The complex rifting and spreading history, as well as the interaction with the Iceland plume,

From: Péron-Pinvidic, G., Hopper, J. R., Stoker, M. S., Gaina, C., Doornenbal, J. C., Funck, T. & Árting, U. E. (eds) 2017. *The NE Atlantic Region: A Reappraisal of Crustal Structure, Tectonostratigraphy and Magmatic Evolution*. Geological Society, London, Special Publications, **447**, 207–231.
First published online July 13, 2016, https://doi.org/10.1144/SP447.1

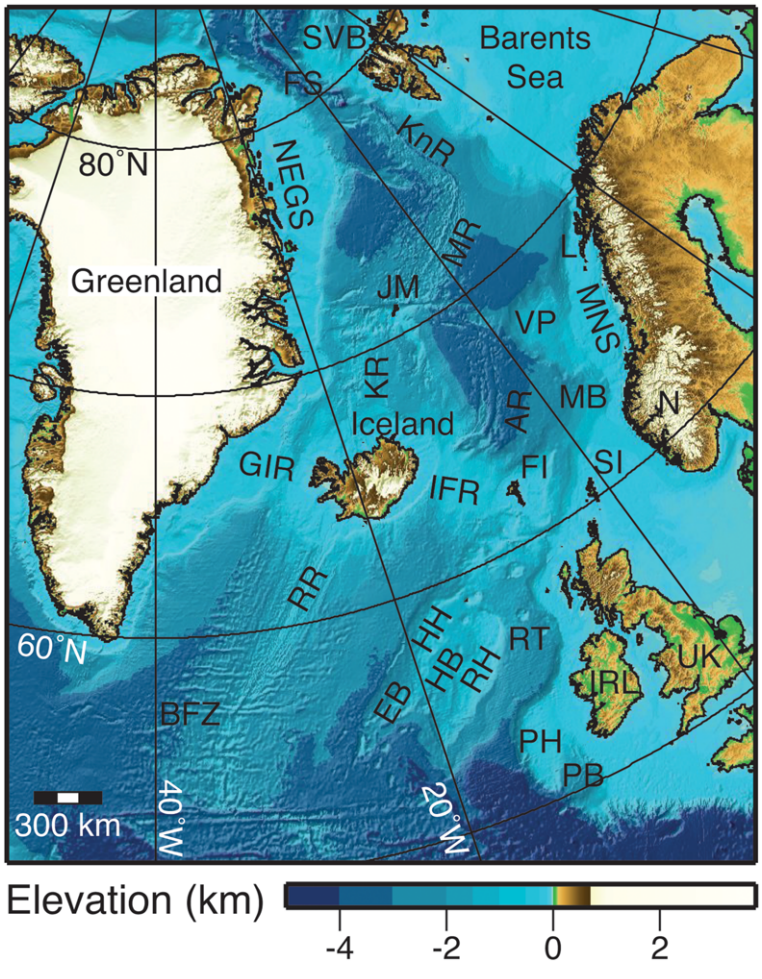

Fig. 1. Physiographical map of the NE Atlantic Ocean using the ETOPO1 Global Relief Model (Amante & Eakins 2009). Abbreviations: BFZ, Bight Fracture Zone; EB, Edoras Bank; FI, Faroe Islands; FS, Fram Strait; GIR, Greenland–Iceland Ridge; HB, Hatton Basin; HH, Hatton High; IFR, Iceland–Faroe Ridge; JM, Jan Mayen; KnR, Knipovich Ridge; KR, Kolbeinsey Ridge; L, Lofoten; MB, Møre Basin; MNS, Mid-Norway Shelf; MR, Mohns Ridge; N, Norway; NEGS, NE Greenland Shelf; PB, Porcupine Basin; PH, Porcupine High; RH, Rockall High; RR, Reykjanes Ridge; RT, Rockall Trough; SI, Shetland Islands; SVB, Svalbard; VP, Vøring Plateau.

have shaped the present configuration of the crust in the NE Atlantic realm. The first-order structure of the crust can be recognized by regional mapping of the Moho and basement depth. A number of maps already exist for the region, such as the global model CRUST1.0 of Laske *et al.* (2013) or the model for the North Atlantic region by Artemieva & Thybo (2013). In addition, large parts of the region are included in compilations that cover the European plate (Grad *et al.* 2009; Molinari & Morelli 2011). In contrast to these existing maps for the NE Atlantic Ocean, the new compilation is exclusively compiled from seismic refraction data supplemented by receiver functions along the bordering land areas. Most seismic refraction lines are acquired along pre-existing multichannel seismic (MCS) data. The interpretation of the MCS data down to the basement is generally used as the starting point for velocity modelling of the seismic refraction lines. Deep crustal seismic reflection data were not considered for two reasons. First, even though the reflection and refraction Moho generally correlate well, there can be deviations (cf. Mooney & Brocher 1987). Second, seismic reflection data require a conversion from time to depth, which is difficult to do when no velocity information is

available. To allow for the best possible quality control and internal consistency, existing local compilations were not incorporated into our database. Examples of such compilations are the seismically constrained gravity inversion for Iceland (Kaban *et al.* 2002) or the model for the Barents Sea (Ritzmann *et al.* 2007) that is based on both seismic reflection and refraction data, as well as on gravity modelling.

By incorporating so far unpublished seismic refraction data, the compilation has an unparalleled data density (Fig. 2), even though there are still substantial data gaps. These unpublished datasets comprise lines that have only been presented at conferences or in internal reports. Knowledge of the basement and Moho depth allows the calculation of the crustal thickness from which stretching factors can be estimated (cf. Kimbell *et al.*, this volume,

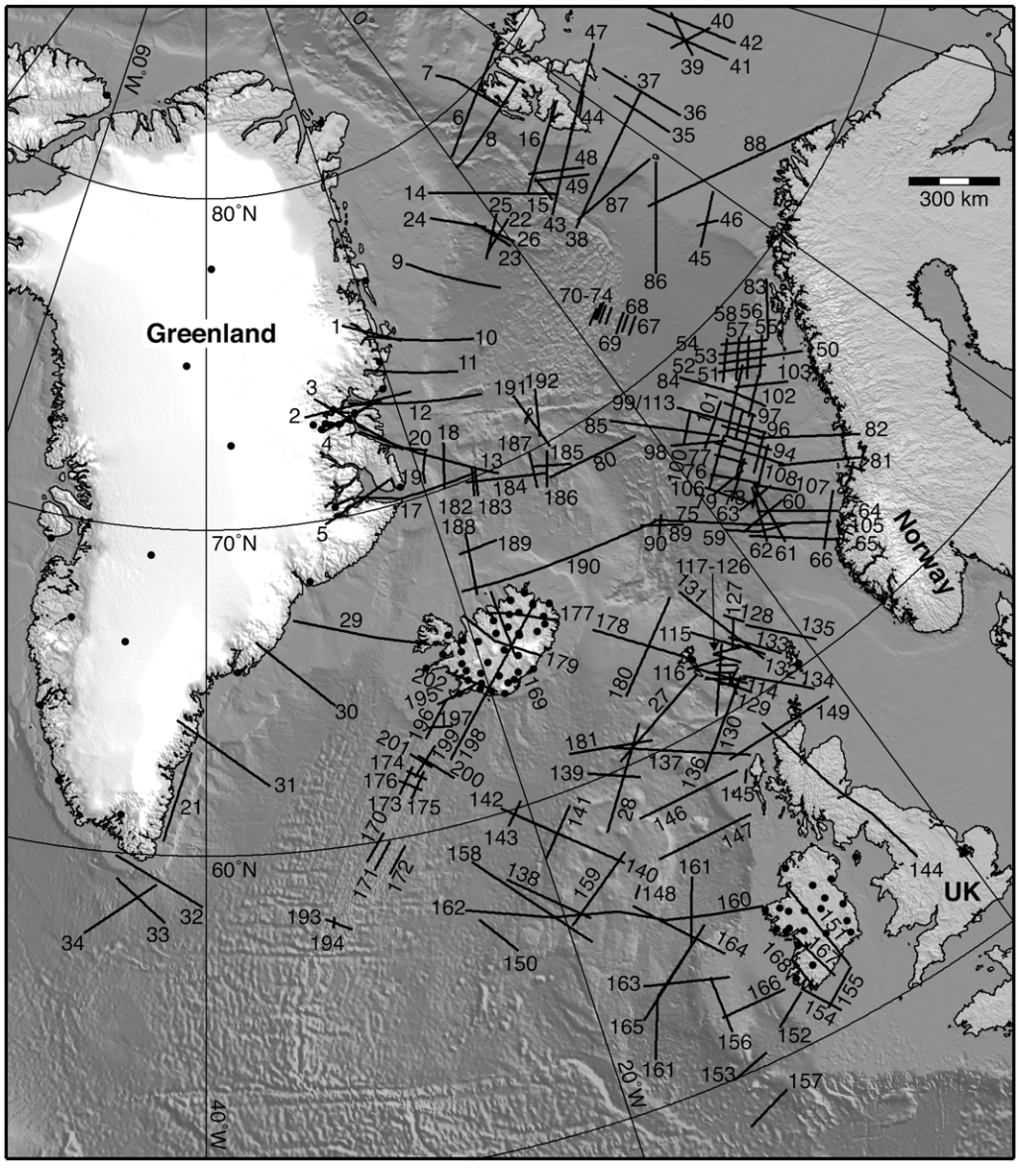

Fig. 2. Data coverage. Solid lines show the location of seismic refraction lines. The labels refer to Table 1 where line names and references are given. Circles mark the positions of receiver functions (see Table 2 for references). The background shows a shaded relief map (ETOPO1: Amante & Eakins 2009).

Table 1. *Seismic refraction studies used in the compilation of data*

Label	Line name	References and comments
1–5	AWI 94300, AWI 94320, AWI 94340, AWI 94360 and AWI 94400	Mandler & Jokat (1998), Schlindwein & Jokat (1999), Schmidt-Aursch & Jokat (2005)
6–8	AWI 99200, AWI 99300 and AWI 99400	Ritzmann & Jokat (2003), Czuba *et al.* (2004, 2005), Ritzmann *et al.* (2004)
9–12	AWI 20030200, AWI 20030300, AWI 20030400 and AWI 20030500	Voss & Jokat (2007, 2009), Voss *et al.* (2009)
13–15	AWI 20090100, AWI 20090200 and AWI 20090250	Jokat (2010), Jokat *et al.* (2012), Hermann & Jokat (2013)
16	AWI 97260 and Barents 98 line 9	Ritzmann *et al.* (2002)
17–20	ARK 1988 lines 3–6	Weigel *et al.* (1995)
21	DLC 94 line 5	Dahl-Jensen *et al.* (1998)
22–24	EAGER 2011 lines 1–3	Gerlings *et al.* (2014), Funck *et al.* (2015)
25–26	GEUS 2002 lines A and B	Døssing *et al.* (2008), Døssing & Funck (2012)
27–28	LOS 2004 lines A and B	Funck *et al.* (2008)
29–32	SIGMA lines 1–4	Korenaga *et al.* (2000), Holbrook *et al.* (2001), Hopper *et al.* (2003), Reiche *et al.* (2011)
33–34	SIGNAL lines 2 and 3	Funck *et al.* (2012)
35–46	Barents 98 lines 1, 2, 3E, 3W, 4–8, 10, A and B	Breivik *et al.* (2002, 2003, 2005), Mjelde *et al.* (2002*b*), Ljones *et al.* (2004)
47	Horsted '05	Czuba *et al.* (2008)
48–49	Knipovich 02 lines 1 and 2	Kandilarov *et al.* (2008, 2010)
50–58	Lofoten 88 lines 1–9	Mjelde (1992), Mjelde *et al.* (1992, 1993, 1995), Mjelde & Sellevoll (1993)
59–63	Møre 99 lines 1–5	Mjelde *et al.* (2009)
64–66	Møre 2009 lines 1–3	Kvarven *et al.* (2014)
67–74	Mohns Ridge 88 lines 2–4 and 6–10	Klingelhöfer *et al.* (2000)
75–80	OBS 2000 lines 1–3, 5, 6 and 8	Breivik *et al.* (2006), Raum *et al.* (2006), Rouzo *et al.* (2006), Mjelde *et al.* (2008)
81–85	OBS 2003 lines 3, 4, 8, 10 and 11	Breivik *et al.* (2008, 2009, 2011) for line 8: Mjelde (pers. comm.)
86–87	OBS 2008 lines 1 and 2	Czuba *et al.* (2011), Libak *et al.* (2012*a*, *b*)
88	PETROBAR 07	Clark *et al.* (2013)
89–90	Valdivia 59–87 lines IV and V	Grevemeyer *et al.* (1997)
91–97	Vøring 92 lines 1–7	Mjelde *et al.* (1997*a*, *b*, 2003), Digranes *et al.* (1998). Note: lines 1, 2, 3 and 5 are not labelled on the map (Fig. 2)
98–112	Vøring 96 lines 1–7, 8A, 8B, 9–14	Mjelde *et al.* (1998, 2001, 2003), Raum (2000), Berndt *et al.* (2001), Raum *et al.* (2002, 2006). Note: lines 7 and 11–14 are not labelled on the map (Fig. 2)
113	Vøring 99 line AB	Mjelde *et al.* (2005, 2007). Note: the line is not labelled on the map (Fig. 2)
114–115	AMG 95 lines 1 and 2	Raum *et al.* (2005)
116	FAST	Richardson *et al.* (1999), Smallwood *et al.* (2001)
117–128	FLARE lines 1–12	Richardson *et al.* (1999), White *et al.* (1999), Fliedner & White (2003), internal reports (Faroese Earth and Energy Directorate)
129–130	Foerbas lines 1 and 2	Internal reports (Faroese Earth and Energy Directorate)
131	iSIMM Faroes	Eccles *et al.* (2007), Roberts *et al.* (2009)
132–133	Mobil lines 1 and 2	Hughes *et al.* (1998), Makris *et al.* (2009)
134–138	AMP lines A, C–E and L	Klingelhöfer *et al.* (2005), Kelly *et al.* (2007), England (pers. comm.)
139	BANS-1	Klingelhöfer *et al.* (2005)
140–143	iSIMM Hatton dip line/strike line/dip line (W)/western strike line	Smith *et al.* (2005), Parkin & White (2008), White & Smith (2009)
144	LISPB	Bamford *et al.* (1977, 1978), Barton (1992)
145	PUMA	Powell & Sinha (1987)

(*Continued*)

Table 1. *Continued*

Label	Line name	References and comments
146–147	BP/Britoil lines 86-002 and 86-005	Roberts *et al.* (1988)
148	Hatton Bank line A	Scrutton (1970, 1972), Bunch (1979)
149	W-reflector profile	Warner *et al.* (1996), Morgan *et al.* (2000), Price & Morgan (2000)
150	CAM 77	Barton & White (1997)
151–155	COOLE lines 1, 3A, 3B, 6 and 7	Makris *et al.* (1988), Lowe & Jacob (1989), O'Reilly *et al.* (1991)
156	Rockall Bank Profile A	Bunch (1979)
157	Goban Spur	Bullock & Minshull (2005), Minshull (pers. comm.)
158–159	HADES combined lines 1 and 2, and line 3	Morewood *et al.* (2005), Ravaut *et al.* (2005), Chabert *et al.* (2006), McDermott (pers. comm.)
160–166	RAPIDS lines 1, 2, 2-1, 32, 33, 34 and 4	Makris *et al.* (1991), Hauser *et al.* (1995), O'Reilly *et al.* (1996), Vogt *et al.* (1998), Shannon *et al.* (1999), Mackenzie *et al.* (2002), Morewood *et al.* (2004, 2005)
167–168	VARNET lines A and B	Masson *et al.* (1998), Landes *et al.* (2000), Hauser *et al.* (2008), O'Reilly *et al.* (2010)
169	B96	Menke *et al.* (1998)
170–172	BK 80 lines X, Y and Z	Bunch & Kennett (1980)
173–176	CAM 71–74	Smallwood *et al.* (1995), Smallwood & White (1998)
177–178	FIRE Land and Offshore	White *et al.* (1996), Staples *et al.* (1997), Richardson *et al.* (1998)
179	ICEMELT	Darbyshire *et al.* (1998, 2000)
180	IFR	Sedov & Makris (2001), Bohnhoff & Makris (2004)
181	IS 2004	Erlendsson & Blischke (2013), Gunnarsson (pers. comm.)
182–187	JMKR-95 lines 1–6	Kodaira *et al.* (1997, 1998*a*, *b*), Mjelde *et al.* (2002*a*)
188–190	KRISE lines 1, 4 and 7	Hooft *et al.* (2006), Furmall (2010), Brandsdóttir *et al.* (2015)
191–192	OBS-JM-2006 lines 1 and 2	Kandilarov *et al.* (2012)
193–194	RAMESSES lines 1 and 2	Navin *et al.* (1998), Sinha *et al.* (1998)
195–197	RISE lines A, B and D	Weir *et al.* (2001)
198–201	RRISP-77 lines 1 and 3–5	Angenheister *et al.* (1980), Gebrande *et al.* (1980), Goldflam *et al.* (1980), Jacoby *et al.* (2007)
202	SIST	Bjarnason *et al.* (1993)

in press). Crustal thickness is also an important parameter for deformable plate reconstructions and basin modelling.

Dataset

The core study area for the mapping of the Moho and basement depth comprises the NE Atlantic Ocean, extending from the Bight Fracture Zone and the southern limit of the Edoras Bank, Rockall and Porcupine highs in the south, to the Fram Strait and western Barents Sea in the north (Fig. 1). While the focus was on the offshore region, Iceland was an integral part of this study.

The primary database behind the compilation consists of velocity–depth models derived from seismic refraction data. Figure 2 shows the location of all lines that were used in this study, and Table 1 provides the line names and references. The 202 lines under consideration were acquired between 1969 and 2011, but only 10 of them prior to 1980. There are numerous other seismic refraction lines in the study area that were not included. The reason for dismissal was mainly associated with age, which frequently was associated with a limited resolution of the velocity models and often the published information would not allow for a proper quality assessment. The majority of lines that were considered in this study were experiments that used ocean-bottom seismometers (either equipped with geophones or hydrophones or both) and seismic land stations as receivers, and airgun arrays or explosives as the source. Occasionally, some additional sonobuoys were used to receive the seismic signals. Only two lines incorporated expanded spread profiles (ESP)

Table 2. *Receiver function studies used in the compilation of data*

Region	References
Greenland	Gregersen *et al.* (1988), Dahl-Jensen *et al.* (2003), Kumar *et al.* (2007), Schiffer *et al.* (2014)
Iceland	Schlindwein (2006), Kumar *et al.* (2007)
Faroe Islands	Harland *et al.* (2009)
Ireland and UK	Tomlinson *et al.* (2006), Licciardi *et al.* (2014)

and 12 lines from the Faeroes Large Aperture Research Experiment (FLARE) (e.g. Fliedner & White 2003) used long-offset seismic lines by towing two multichannel streamers with maximum offsets of 38 km.

The secondary dataset used in this study consisted of receiver functions analysis. This method was based on the observation of teleseismic events at either permanent or temporary deployed stations. Receiver function analysis provides information on the depth of the Moho beneath the station and can fill in some gaps in the primary dataset. Regions of particular interest were Iceland, Greenland and Ireland. Table 2 provides information on the receiver function studies used in the compilation, while the station location is shown in Figure 2.

Compilation

The database consisting of the velocity models from the seismic refraction lines and the Moho depths from the receiver function studies was used to compile both the depth to the basement and the depth to the Moho in the NE Atlantic Ocean. The Moho is generally characterized by an increase in P-wave velocity to values greater than 7.6 km s^{-1} (White *et al.* 1992). This increase is often associated with a prominent wide-angle reflection (PmP). However, serpentinization processes in the mantle rock can reduce the seismic velocity to values as low as 4.8 km s^{-1} (Christensen 2004). In these cases, the Moho depth is measured at the top of the (partially) serpentinized mantle.

For the definition of basement, the top of the igneous crust is used in the oceanic domain. Landwards of the continent–ocean boundary, basement is measured at the top of the crystalline crust. That way, any volcanic rocks located above the continental crystalline crust are considered as part of the sedimentary column. Off NE Greenland, the top of the crystalline crust could not be resolved on some of the lines owing to the presence of consolidated Palaeozoic and Mesozoic sedimentary rocks with velocities exceeding 5 km s^{-1} and a lack of a clear seismic discontinuity at the basement. These lines include AWI 20030200 (Voss *et al.* 2009), AWI 20030300 (Voss *et al.* 2009), AWI 20030400 (Voss & Jokat 2007) and AWI 20030500 (Voss & Jokat 2007, 2009), and here the 5.7 km s^{-1} velocity contour was used as a proxy for the basement. This value differs from the commonly assumed 6.0 km s^{-1} velocity contour as the base of sediments, as the existing data indicate that the crystalline Caledonian basement both in East Greenland and in northern Svalbard can display P-wave velocities down to 5.5 km s^{-1} (Schmidt-Aursch & Jokat 2005; Czuba *et al.* 2005). Therefore, we used the 5.7 km s^{-1} contour as a compromise to avoid an overestimation of the sedimentary thickness.

The original digital velocity models and navigation data were obtained for a majority of the seismic refraction lines, thus avoiding possible inaccuracies that result from digitizing figures from papers. For the compilation of the basement map, only the portions of the lines with seismic control on the basement depth were used. In the next step, the misfit at the cross-points was investigated. In the case of misfits, the original velocity models and the underlying documentation were revisited to check the basement constraints. Data in the vicinity of the cross-point was then excluded along the line with the poorer constraints.

In the case of Iceland, the basement is mostly equivalent to the topography, with exception of areas that are covered by glaciers and thin sediments (mostly beach sands). The existing seismic refraction lines on Iceland often use simplified versions of the topography as the large shot and receiver spacing makes it unnecessary to take the small-scale topographical variations into account. In addition, there are a number of shot and receiver positions that are projected onto the seismic lines, which introduces erroneous elevations. For this reason, the basement points in Iceland and the adjacent coastal zone (see the extent in Fig. 3) were removed from the dataset and replaced with the ETOPO1 Global Relief Model (Amante & Eakins 2009). Regions with glaciers and beach sands were not assigned a basement depth.

All data points were converted to a Lambert conformal projection with 40°W as the central meridian, and 55°N and 75°N as standard parallels. Along the seismic lines, the basement depth was sampled at a spacing of 1 km. Together with the basement points around Iceland, a basement map was compiled employing the universal kriging technique (Stein 1999). Prior to this, a block mean with a point spacing of 10 km was applied to maintain lateral resolution in areas with dense line spacing, such as along the Norwegian margin. Universal kriging within the SAGA GIS tool (Böhner & Antonić

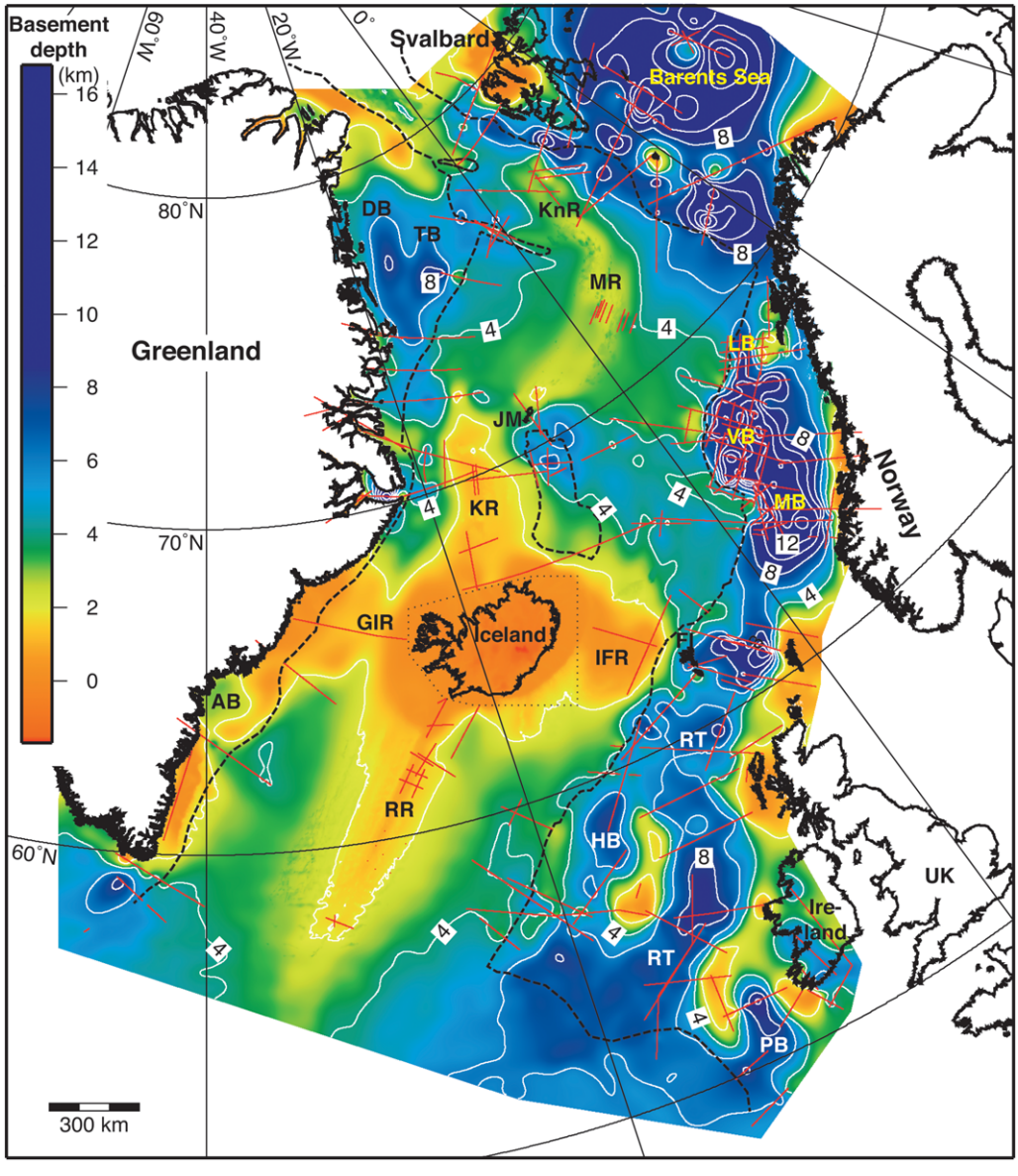

Fig. 3. Basement depth (below sea level). White lines show the contours with a 2 km interval. Seismic constraints are shown in red. Within the dotted line around Iceland, the basement is approximated by the topography. The dashed line indicates the continent–ocean boundary (Funck *et al.* 2014). Abbreviations: AB, Ammassalik Basin; DB, Danmarkshavn Basin; FI, Faroe Islands; GIR, Greenland–Iceland Ridge; HB, Hatton Basin; IFR, Iceland–Faroe Ridge; JM, Jan Mayen; KnR, Knipovich Ridge; KR, Kolbeinsey Ridge; LB, Lofoten Basin; MB, Møre Basin; MR, Mohns Ridge; PB, Porcupine Basin; RR, Reykjanes Ridge; RT, Rockall Trough; TB, Thetis Basin; UK, United Kingdom; VB, Vøring Basin.

2008; Olaya & Conrad 2008) was applied using free-air gravity as a constraint for the interpolation and extrapolation. The gravity data were obtained from the DTU10 grid (Andersen *et al.* 2010; see also fig. 1b in Haase *et al.*, this volume, in review). Owing to the lack of seismic constraints, the onshore areas – with the exception of Iceland, western Ireland, Svalbard, the Faroe Islands and some other smaller islands – were clipped from the resulting basement map shown in Figure 3.

For the compilation of the Moho depth, velocity models along the seismic refraction lines were reviewed to reject portions of the profiles on which the Moho is not constrained by Moho reflections (PmP) or mantle refractions (Pn). Not all publications display the ray coverage to assess the model constraints. In these cases, the outer portions of the models were excluded. The consistency checks at the cross-points of the lines were performed the same way as for the basement depth. Two lines were completely removed from the Moho dataset. The first line is the IFR profile (Bohnhoff & Makris 2004) across the Iceland–Faroe Ridge, which has a substantially lower Moho depth (23 km) than the FIRE offshore line (Richardson *et al.* 1998) along the ridge (>30 km) (Fig. 4). Given that the SIGMA line 1 (Holbrook *et al.* 2001) on the conjugate Greenland–Iceland Ridge displays Moho depths greater than 30 km, the IFR profile was eliminated from the Moho dataset.

The second dataset to be dismissed was DLC 94 line 5 (Dahl-Jensen *et al.* 1998) along the SE coast of Greenland. Along this line, the Moho depth varies between 39 and 52 km, which is substantially more than the maximum Moho depth of 33 km on the two nearby lines 3 (Hopper *et al.* 2003) and 4 (Holbrook *et al.* 2001) of the SIGMA experiment. DLC 94 line 5 has a difficult geometry, with a crooked shot line along the coast and only three receivers onshore. Hence, there might be out-of-plane phases mimicking a Moho. Alternatively, the deep Moho could be an intra-mantle reflection similar to the one observed off West Greenland (Gerlings *et al.* 2009) in an area that was affected by the Iceland plume. The depth at the top of the high-velocity zone (7.5 km s^{-1}) on DLC 94 line 5 varies between 26 and 34 km, and would, in fact, be in reasonable agreement with the interpreted Moho on SIGMA lines 3 and 4.

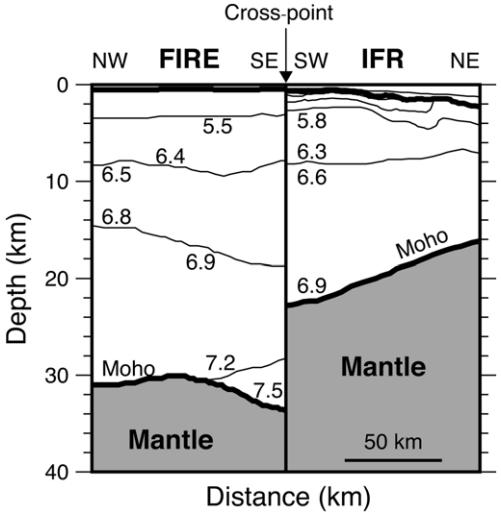

Fig. 4. Comparison of P-wave velocity models of the intersecting seismic refraction lines FIRE Offshore (Richardson *et al.* 1998) and IFR (Bohnhoff & Makris 2004) on the Iceland–Faroe Ridge. Velocities are specified in km s^{-1}.

Moho depths obtained from receiver functions were reviewed critically before they were added to the database. Of particular concern were the measurements on Iceland, as Schlindwein (2006) pointed out that the P–S converted phases there are only weak, which is why the use of the receiver function technique may be limited. For this reason, the 53 available measurements by Kumar *et al.* (2007) were cross-checked with the seismic refraction data and the seismically controlled gravity inversion of Kaban *et al.* (2002). In this process, 14 receiver functions were rejected, as they were not consistent with the other methods. Most of the excluded stations are located close to the coast.

West of the main mapping area, the cleaned dataset of Moho points was supplemented with the global crustal model of Laske *et al.* (2013) at a resolution of 1° (Fig. 5). In the east, the dataset was extended with the European Moho map of Grad *et al.* (2009) at a resolution of 0.1° (Fig. 5). The available computational power required a resampling of the European Moho on a 50 km raster in the Lambert projection described above. To equalize the data distribution, a block average filter was applied to the entire dataset using a 10 km raster. The Moho map (Fig. 6) was then interpolated using the SAGA GIS tool Global Ordinary Kriging. The variance in the logarithmic form was used as a quality measure and the inverse distance was applied as an interpolation method. Finally, the crustal thickness (Fig. 7) was calculated from the difference between the Moho and basement depth.

Results

The basement, Moho and crustal thickness maps compiled from the seismic data are shown in Figures 3, 6 and 7, respectively. A brief description of the main observations is given in this section, while some features of the maps are discussed in more detail in the following section.

On the basement map (Fig. 3), the Greenland–Iceland–Faroe Ridge stands out as a zone of elevated basement. On the Greenland–Iceland Ridge, the maximum basement depth along SIGMA line 1 is 1.6 km below sea level (Holbrook *et al.* 2001). In Iceland, the basement is above sea level and the adjacent mid-oceanic spreading ridges (the

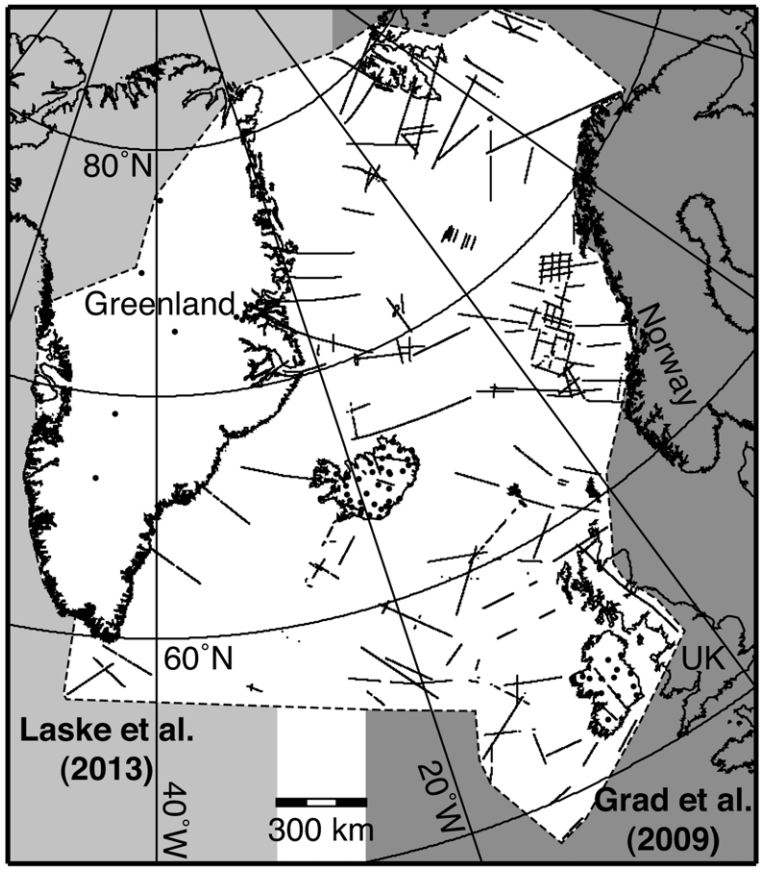

Fig. 5. Datasets used for the compilation of the Moho depth. Circles and lines show the receiver functions and seismic refraction lines, respectively.

Reykjanes and Kolbeinsey ridges) are also characterized by elevated basement. However, the basement depth on these ridges increases with increasing distance from Iceland.

Another prominent feature on the basement map (Fig. 3) is the continuous basin along the NW European margin that extends from the southern Rockall Trough to the Lofoten Basin. The maximum basement depth in this zone is 15 km in the Møre and Vøring basins off mid-Norway. The SW Barents Shelf is also characterized by a deep basement, often exceeding 8 km in depth and up to a maximum depth of 17 km. The sedimentary basins off East Greenland are not well covered by seismic refraction profiles, but there is an indication for basement depths exceeding 8 km off NE Greenland. A smaller basin in the south (the Ammassalik Basin) will be discussed below.

Similar to the basement map, the Greenland–Iceland and Iceland–Faroe ridges are very prominent on the depth to Moho map (Fig. 6). The minimum Moho depth on these ridges is 29 km, while the maximum Moho depth beneath Iceland is 39 km. South and north of Iceland, the Moho is generally shallowest along the spreading ridges (5–10 km) from where the Moho deepens towards the continent–ocean boundary (15–20 km). This increase in Moho depth is related to the cooling of the lithosphere with age and to excess magmatism around the time of break-up, which resulted in anomalously thick oceanic crust close to the continent–ocean boundary (Holbrook *et al.* 2001). The basins along the NW European margins are associated with a relatively shallow Moho depth, best seen in the Rockall Trough (12 km) and the Porcupine Basin (10 km).

Onshore Greenland, the Moho is deepest in the southern part with a depth of 40–45 km, while the NW part displays depths of 35–40 km (Fig. 6). In NW Europe, the deepest Moho in the mapping area is found in Scandinavia (47 km: Grad *et al.* 2009). In Ireland and the UK, the Moho is

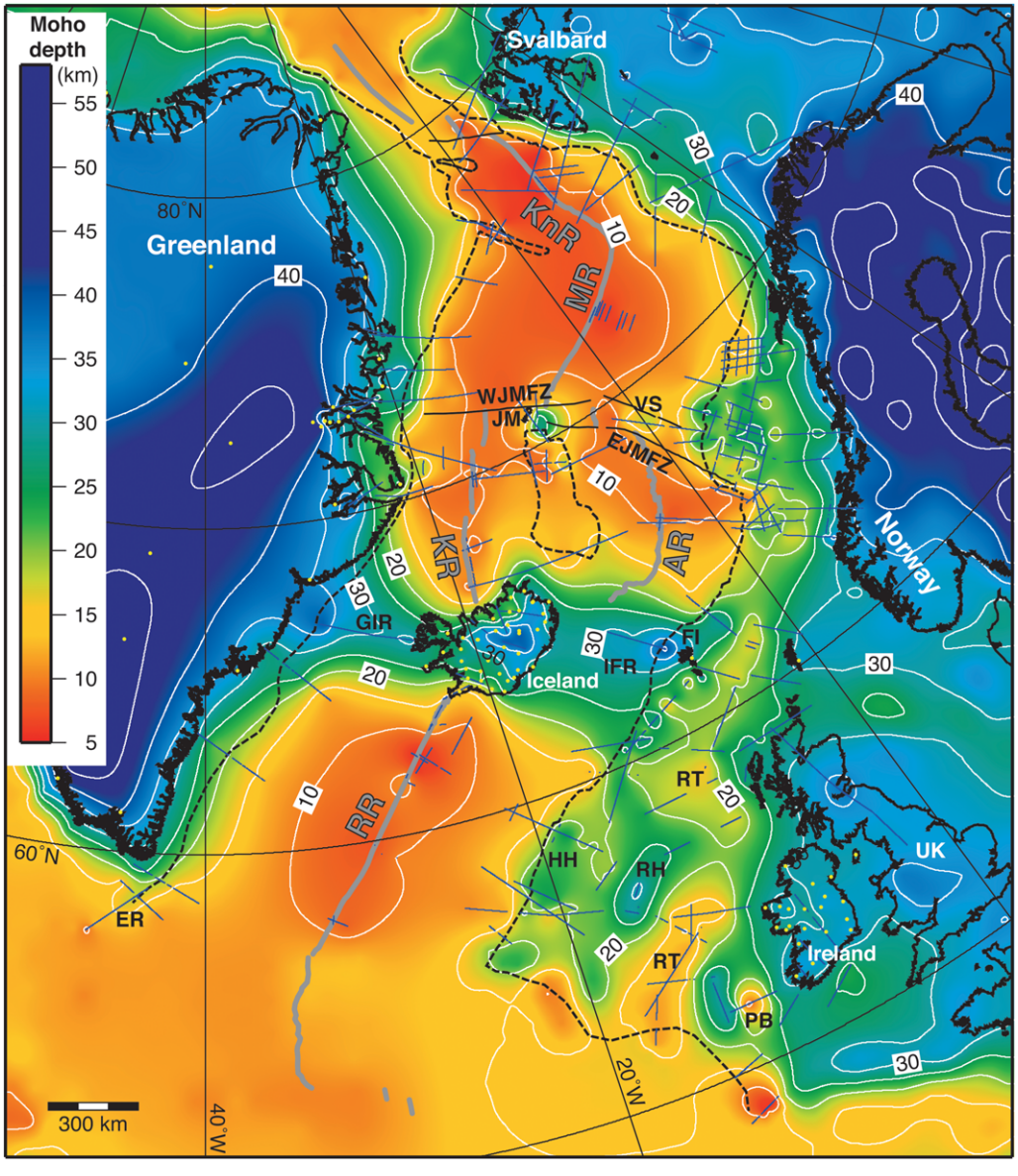

Fig. 6. Moho map (depth below sea level). White lines show the contours with a 5 km interval. Solid lines and yellow circles mark the location of seismic refraction data and receiver functions, respectively. The dashed line indicates the continent–ocean boundary (Funck *et al.* 2014). Grey lines mark active and extinct spreading ridges. Abbreviations: AR, Aegir Ridge; EJMFZ, East Jan Mayen Fracture Zone; ER, Eirik Ridge; FI, Faroe Islands; GIR, Greenland–Iceland Ridge; HH, Hatton High; IFR, Iceland–Faroe Ridge; JM, Jan Mayen; KnR, Knipovich Ridge; KR, Kolbeinsey Ridge; MR, Mohns Ridge; PB, Porcupine Basin; RR, Reykjanes Ridge; RH, Rockall High; RT, Rockall Trough; UK, United Kingdom; VS, Vøring Spur; WJMFZ, West Jan Mayen Fracture Zone.

substantially shallower, varying mainly between 30 and 36 km.

The crustal thickness map (Fig. 7) displays similar characteristics to the Moho map (Fig. 6). The Greenland–Iceland–Faroe Ridge has a minimum thickness of 28 km. South of the ridge, the thickness of the oceanic crust varies mostly between 5 and 8 km, not too dissimilar from the average oceanic crust thickness of 7 km (White *et al.* 1992). North of Iceland, the crust produced along the Kolbeinsey

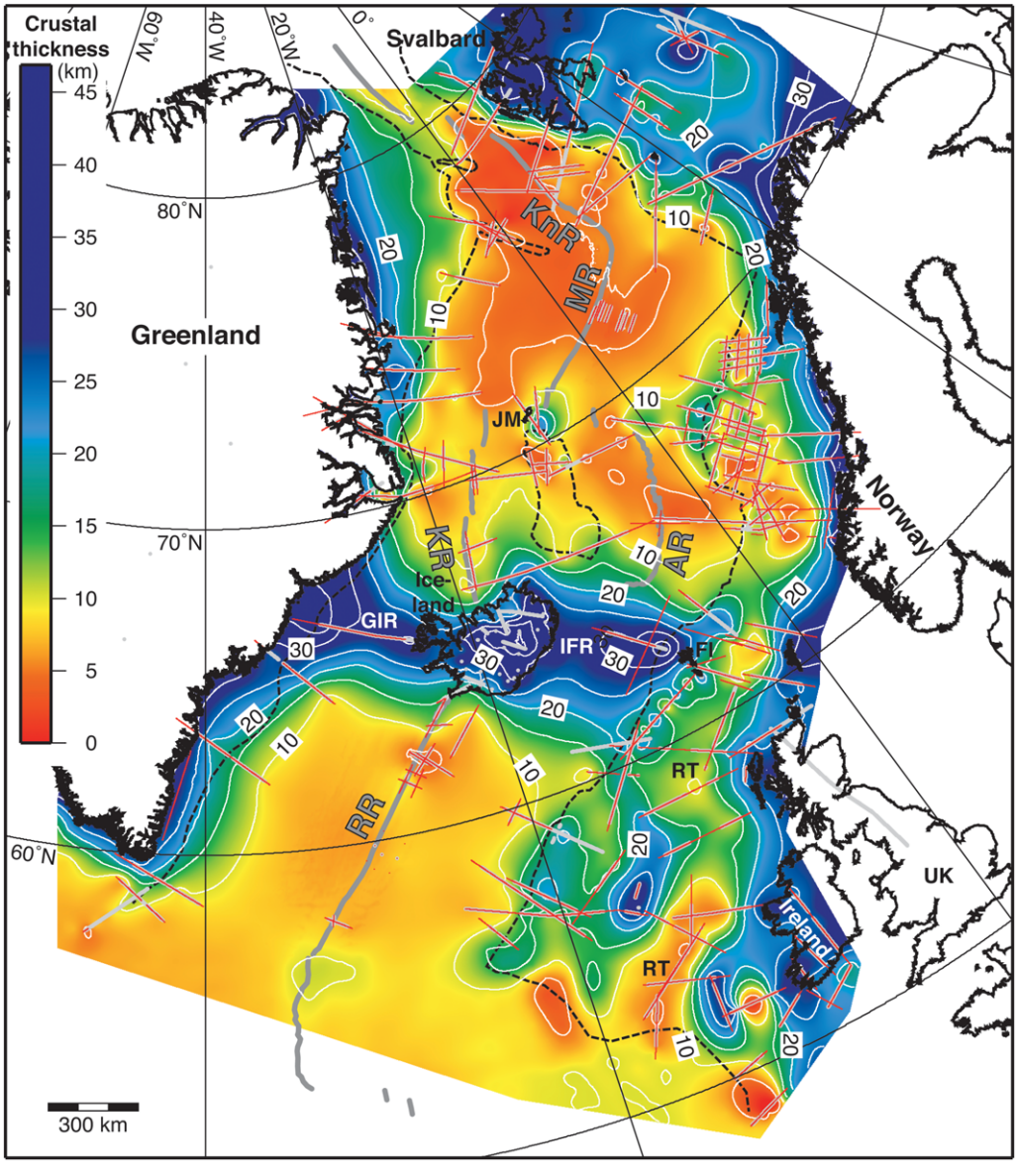

Fig. 7. Crustal thickness map with a contour interval of 5 km (white lines). Data points with Moho and basement constraints are shown in grey and red, respectively. The dashed line indicates the continent–ocean boundary (Funck *et al.* 2014). Grey lines mark active and extinct spreading ridges. Abbreviations: AR, Aegir Ridge; FI, Faroe Islands; GIR, Greenland–Iceland Ridge; IFR, Iceland–Faroe Ridge; JM, Jan Mayen; KnR, Knipovich Ridge; KR, Kolbeinsey Ridge; MR, Mohns Ridge; Reykjanes Ridge; RT, Rockall Trough; UK, United Kingdom.

Ridge is around 8 km thick (e.g. Kodaira *et al.* 1997), while the crust that formed at the now extinct Aegir Ridge is mostly thinner than 6 km (e.g. Breivik *et al.* 2006). Further north along the Mohns Ridge, crustal thickness decreases to 4–5 km (Klingelhöfer *et al.* 2000), and along the Knipovich Ridge segment, the thickness varies between 3 km (Hermann & Jokat 2013) and 7 km (Kandilarov *et al.* 2010).

Within the Rockall Trough, the crust thickens from 5 km in the south to 10 km in the north (Fig. 7). Further to the north, within the Faroe–Shetland Trough, the thickness of the crystalline crust thins again to values as small as 7 km (Makris

et al. 2009). Likewise, the basins off mid-Norway are characterized by a thin crust with a minimum thickness of 5 km (e.g. Raum 2000).

Discussion

Conjugate margin comparison

The maps displaying basement depth (Fig. 3), Moho depth (Fig. 6) and crustal thickness (Fig. 7) are compiled from seismic refraction data that are unevenly distributed across the study area (Fig. 2). In particular, the NW European margin is much better sampled with seismic data when compared to the East Greenland continental margin. This offers the opportunity to learn from NW Europe when studying the structures found along the East Greenland coast. At the same time, the conjugate margin comparison can reveal potential shortcomings of the compilation that result from the distribution or interpretation of data.

Along the SE Greenland margin, the Ammassalik Basin shows up as a 3 km-deep basement low (Fig. 3). The structure is not sampled by seismic refraction data, but was introduced by the kriging algorithm that used free-air gravity (Andersen *et al.* 2010) as a constraint. Hence, the basin outline correlates with the corresponding gravity low in that area. There are few seismic reflection data available that could independently confirm the shape and depth of the basin. Hopper *et al.* (1998) were the first to notice the presence of a sedimentary basin in this region: they interpreted the structure as a rift system with a sediment infill corresponding to 1 s two-way travel time (TWT). Reprocessing of the seismic data suggests a probable sediment thickness of at least 3 km (Gerlings *et al.*, this volume, in review).

When the basement depth is reconstructed for Chron C24 (Fig. 8) using the rotation poles of Gaina (2014), the Ammassalik Basin lies just to the north of the Anton Dohrn Lineament Complex at the conjugate NW European margin. Kimbell *et al.* (2005) identified three individual lineaments within this complex. The continent–ocean boundary is shifted landwards across the complex (when moving from south to north), while the axis of the Rockall Trough is offset seawards by some 200 km. The Hatton Basin does not continue northwards of the Anton Dohrn Lineament Complex. This is why the Ammassalik Basin could be a NW-shifted continuation of the Hatton Basin that was left on the Greenland side at the time of final break-up. This shift would essentially be similar to the one observed between the northern and southern Rockall Trough. Hence, knowledge of the poorly studied Ammassalik Basin can probably be increased by comparison to the Hatton Basin.

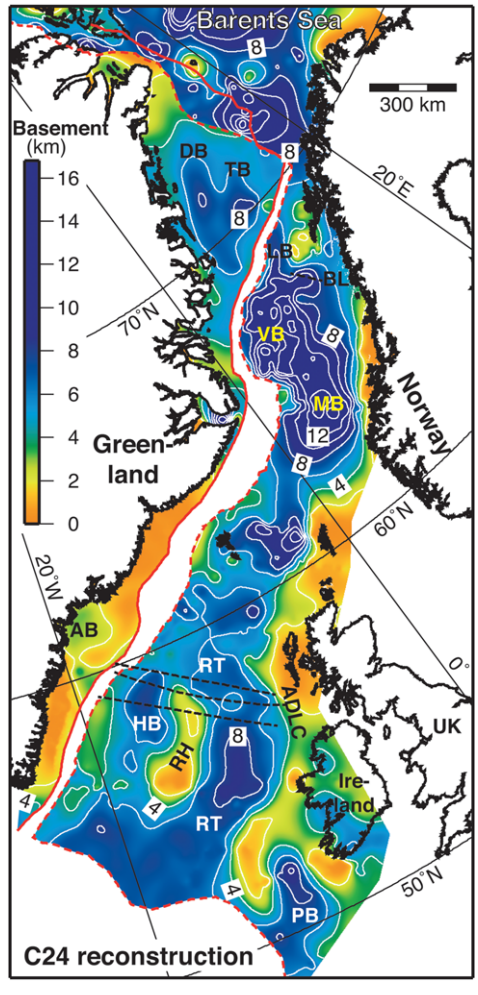

Fig. 8. Reconstruction of the basement depth for Chron C24 using the rotation pole of Gaina (2014). Europe is fixed in this reconstruction and the rotation of Greenland is carried out with GMT (Generic Mapping Tools) software (Wessel *et al.* 2013). White lines show the contours with a 2 km interval. The solid and dashed red lines mark the continent–ocean boundary (COB) of Greenland and NW Europe, respectively (Funck *et al.* 2014). Note that there is an overlap of the COB in the northernmost area. Dashed lines indicate lineaments. Abbreviations: AB, Ammassalik Basin; ADLC, Anton Dohrn Lineament Complex; BL, Bivrost Lineament; DB, Danmarkshavn Basin; HB, Hatton Basin; LB, Lofoten Basin; MB, Møre Basin; PB, Porcupine Basin; RH, Rockall High; RT, Rockall Trough; TB, Thetis Basin; UK, United Kingdom; VB, Vøring Basin.

In the Hatton Basin, the total sediment thickness is more than 6 km in the northern part (Hopper *et al.*, this volume, in prep) and this could be an indication

of the possible depth of the Ammassalik Basin. Hence, the kriging technique with gravity as a constraint may underestimate the basement depth if seismic data are lacking.

Such an underestimation of basement depth also occurs on the NE Greenland continental shelf. The basement reconstruction for Chron C24 (Fig. 8) shows that the deep basins off mid-Norway (the Møre, Vøring and Lofoten basins) correlate with the basins off NE Greenland (the Danmarkshavn and Thetis basins). However, the Norwegian basins are up to 15 km thick, while the maximum depth off Greenland seems to be only 8 km. The seismic refraction constraints within the basins off NE Greenland are restricted to the southern edge of the Danmarkshavn Basin (line AWI 20030300) and the eastern edge of the Thetis Basin (line AWI 20030200) (Fig. 3). In addition, the basement on these two lines is only poorly resolved by the seismic data and is therefore approximated by the 5.7 km s^{-1} velocity contour. Newly released seismic reflection data indicate a maximum sediment thickness of 18 km (Hopper *et al.*, this volume, in prep), which is in better agreement with the mid-Norwegian basins and also with the SW Barents Sea.

While the gravity constraints used in the kriging procedure could outline the general structure of the basins not covered by seismic refraction data, this method seems to underestimate the basement depth, as seen in the two examples from Greenland. Initially, gravity constraints were also tested for the kriging of the Moho depth. In particular, filtered versions of the Bouguer gravity anomaly were used for this purpose. However, these resulted in some features, such as crustal roots, that were difficult to explain in some cases. This is why the final kriging of the Moho was performed without gravity constraints. Instead, regional and global datasets (Grad *et al.* 2009; Laske *et al.* 2013) were used to constrain the surrounding areas. Assuming isostasy, the basins on the continental shelves should be associated with a shallowing of the Moho. While this is the case for basins covered with seismic data (e.g. the Rockall Trough), the basins off Greenland (the Ammassalik, Danmarkshavn and Thetis basins) do not show a corresponding expression in the Moho depth. In these areas, the Moho depth obtained from seismically controlled gravity inversion (Haase *et al.*, this volume, in review) provides greater structural detail.

Thickness of oceanic crust

The oceanic crust in the NE Atlantic Ocean displays variations in thickness ranging between 2 and 40 km (Fig. 9) compared to an average of 7 km for normal oceanic crust (White *et al.* 1992). Areas with thick oceanic crust can generally be related to an increased magmatism associated with the Iceland plume. The Greenland–Iceland–Faroe Ridge is characterized by a 28–40 km-thick crust, which White (1997) interpreted as the interaction of a rising mantle plume with a spreading ridge. He suggested that the thickness variations were related to variations in the temperature of the mantle or mantle flow rates, or both.

South of Iceland, the initial oceanic crustal thickness at break-up is generally greater than 15 km (Fig. 9) and decreases with increasing distance from the plume (cf. Holbrook *et al.* 2001). Over time, the thickness of the oceanic crust decreased to values of around 8 km at a distance of 250 km from the continent–ocean boundary. Refraction seismic experiments on the Reykjanes Ridge away from Iceland indicate variations in the crustal thickness that ranged from 4 to 9 km (Bunch & Kennett 1980; Smallwood *et al.* 1995; Navin *et al.* 1998; Smallwood & White 1998; Jacoby *et al.* 2007).

North of Iceland, the initial spreading after break-up was along the Aegir Ridge, which lasted until 30 Ma when spreading there became extinct (Gaina *et al.* 2009). At that time, the Kolbeinsey Ridge started to develop from the south, with final detachment of the Jan Mayen microcontinent from East Greenland occurring at 20 Ma (Chron C6b) (Gaina *et al.* 2009; Peron-Pinvidic *et al.* 2012). The thickness of the oceanic crust that was formed in the northern portions of the Aegir and Kolbeinsey ridges differs significantly (Fig. 9). Between the Jan Mayen microcontinent and mid-Norway, the initial crustal thickness at break-up was around 11 km (Breivik *et al.* 2006), which is less than that observed in SE Greenland at a similar distance from the Iceland plume (19 km: Hopper *et al.* 2003). Close to the extinct Aegir Ridge, the crustal thickness is as little as 4 km (Breivik *et al.* 2006). In contrast, the crust at the Kolbeinsey Ridge has a thickness of between 7 and 10 km (Kodaira *et al.* 1997). Breivik *et al.* (2006) speculated that the thin oceanic crust between the Jan Mayen microcontinent and mid-Norway is caused by interaction with the Iceland plume. They suggested that the construction of the magmatic Greenland–Iceland–Faroe Ridge to the south depleted the mantle. Asthenospheric flow transported this depleted mantle to the Aegir Ridge, giving a lower than normal magma productivity. Howell *et al.* (2014) employed three-dimensional (3D) numerical models that simulated a plume interacting with rifting continents and spreading ridges. Their results support a plume with a relatively low flux (95–128 m^3 s^{-1}) to explain the restriction of the relatively thick crust in the southern part of the Aegir Ridge.

The Kolbeinsey Ridge terminates at the West Jan Mayen Fracture Zone. Northwards of the fracture

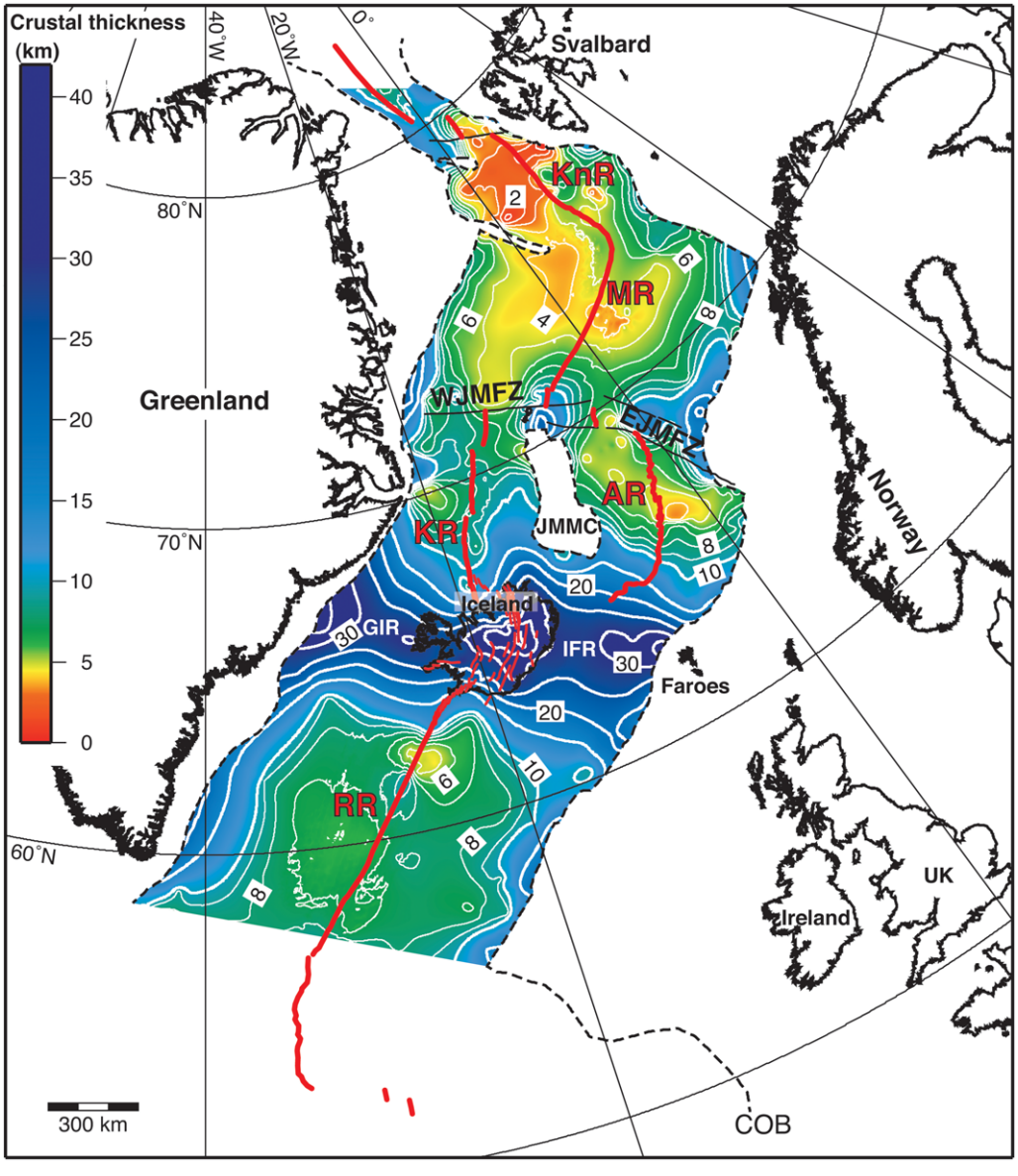

Fig. 9. The thickness of oceanic crust. Contours from 2 to 8 km are shown as thin white lines with an interval of 2 km. Bold white lines are contours >10 km, where a contour interval of 5 km is used. The continent–ocean boundary (COB) is marked by a dashed line. Red lines indicate active and extinct spreading ridges. Abbreviations: AR, Aegir Ridge; EJMFZ, East Jan Mayen Fracture Zone; GIR, Greenland–Iceland Ridge; IFR, Iceland–Faroe Ridge; JMMC, Jan Mayen microcontinent; KnR, Knipovich Ridge; KR, Kolbeinsey Ridge; MR, Mohns Ridge; RR, Reykjanes Ridge; WJMFZ, West Jan Mayen Fracture Zone.

zone, the crustal thickness decreases markedly (Fig. 9). The Mohns Ridge produced thicker than normal oceanic crust just after break-up, but most of the younger crust is only between 4 and 6 km thick. The main exception is the southernmost part of the Mohns Ridge, which is affected by the volcanism on the Jan Mayen islands. Rickers *et al.* (2013) could identify two distinct low-velocity zones in the mantle: one centred beneath Iceland and one beneath the northern Kolbeinsey Ridge. At depth, the latter anomaly covers the whole length of the Kolbeinsey Ridge and extends beyond the

West Jan Mayen Fracture Zone to the southern Mohns Ridge. Just to the north of the West Jan Mayen Fracture Zone, close to Jan Mayen, the crustal thickness is 10 km (Kandilarov *et al.* 2012). Based on the distinct mantle velocity anomalies, Rickers *et al.* (2013) see two seperate hotspots beneath Iceland and Jan Mayen, which can be also supported by isotope studies (Schilling *et al.* 1999).

On a series of seismic refraction lines on the eastern flank of the Mohns Ridge, Klingelhöfer *et al.* (2000) modelled a mean crustal thickness of 4 km that was produced at a full spreading rate of 14 mm a^{-1}. For spreading rates greater than 20 mm a^{-1}, there is little variation in crustal thickness: however, the thickness drops rapidly for lower rates (Dick *et al.* 2003). Crust that was produced at the Knipovich Ridge (a full spreading rate of 14 mm a^{-1}: DeMets *et al.* 1990, 1994) is often just 3 km thick (Hermann & Jokat 2013), in particular to the west of the present location of the ridge. To the east, the crust is generally slightly thicker. Even though there are some asymmetries in crustal accretion at the Knipovich Ridge (Gaina 2014), a systematic difference in crustal thickness on either side of the ridge is difficult to explain. This is why it is worthwhile revisiting the datasets on which the crustal thickness compilation is based.

The main profile that is constraining the crustal thickness west of the Knipovich Ridge is line AWI 20090200 (labelled as number 14 in Fig. 2) (Hermann & Jokat 2013). This line displays a 2–3 km-thick oceanic crust (Fig. 10) that lacks a distinct oceanic layer 3 (Hermann & Jokat 2013). Some 30 km to the south, another profile extends from the Knipovich Ridge towards the NE (Barents 98 line 8, labelled as number 43 in Fig. 2). Close to the ridge, this line exhibits 6–7 km-thick crust (Fig. 10) with distinct oceanic layers 2 and 3 (Ljones *et al.* 2004). A further profile in close proximity is Knipovich 02 line 1 (labelled as numbers 48 in Fig. 2) (Kandilarov *et al.* 2008). Here, the crust is 4 km thick adjacent to the ridge (Fig. 10), which is in better agreement with line AWI 20090200. However, Kandilarov *et al.* (2008) also interpreted the presence of an oceanic layer 3, in contrast to the model of line AWI 20090200 (Hermann & Jokat 2013), on the western side of the Knipovich Ridge. Although crust formed at ultraslow-spreading ridges can display large variations in thickness and velocity structure (Jokat *et al.* 2003; Minshull *et al.* 2006), some differences may also result from different approaches in the velocity modelling and the subsequent interpretation of the model. This is why the three lines will be briefly reviewed here.

The total thickness of oceanic layer 2 is similar on lines AWI 20090200 and Barents 98 line 1 (Fig. 10), even though the level of detail in the models is different. On the AWI line, Hermann & Jokat (2013) differentiated three sublayers (2A, 2B and 2C), while no such subdivision is seen on Barents 98 line 8 (Ljones *et al.* 2004). However, the velocity range observed within layer 2 is not too dissimilar. The main difference here is that the AWI line resolves velocities as low as 2.7 km s^{-1} at the top of the oceanic crust that are not resolved on Barents 98 line 8.

The potentially critical issue on Barents 98 line 8 is the interpreted oceanic layer 3 (Ljones *et al.* 2004) with velocities of 6.4–6.9 and 7.2 km s^{-1} in layers 3A and 3B, respectively (Fig. 10). Ljones *et al.* (2004) stated that there were a total of 107 travel time picks for reflections between layers 2 and 3A, while only 11 Moho reflections (PmP) were picked. With a shot spacing of 200 m, these 11 picks correspond to a 2 km-long segment along which the PmP is observed. With such a limited number of observations, the Moho appears not to have been mapped reliably by reflections. In contrast, the numerous observed reflections between layers 2 and 3 are also unusual, as this is commonly not a reflective boundary. Minshull *et al.* (2006) did not report a single such reflection in their dataset from the ultraslow-spreading SW Indian Ridge, and the same is true for the Mohns Ridge (Klingelhöfer *et al.* 2000). However, both of these other studies show frequent reflections from the Moho. This is why an alternate explanation for the interpreted layer 3 should be looked into. Instead of having a gabbroic composition, a partially serpentinized mantle rock may explain the seismic observations.

The Moho interpretation on line AWI 20090200 is also unclear. Despite a modelled velocity contrast of >1.5 km s^{-1} (Fig. 10), not a single Moho reflection is observed in a 140 km-wide zone adjacent to the Knipovich Ridge (Hermann & Jokat 2013). Hence, there might not be a sharp Moho, as indicated in the model, but rather a gradual velocity transition from layer 2C into the mantle. In this case, the interpreted layer 2C or parts of it could, in fact, be a highly serpentinized mantle. Nevertheless, there are some large misfits between the observed and calculated travel-time curves along the AWI line. For example, ocean-bottom seismometer (OBS) 216 close to the Knipovich Ridge (fig. 2c in Hermann & Jokat 2013) shows that the calculated travel times of the mantle refraction are up to 300 ms too fast, which could mean that the Moho locally could be up to 1.8 km deeper than shown in the velocity model.

When the AWI profile is compared with the Knipovich 02 line 1 (Fig. 10), there is a good match between the combined layers 2A and 2B on line AWI 20090200 (Hermann & Jokat 2013), and oceanic layer 2 on the Knipovich 02 line 1 (Kandilarov *et al.* 2008). This applies to both layer thickness and velocities. The underlying layer is interpreted as

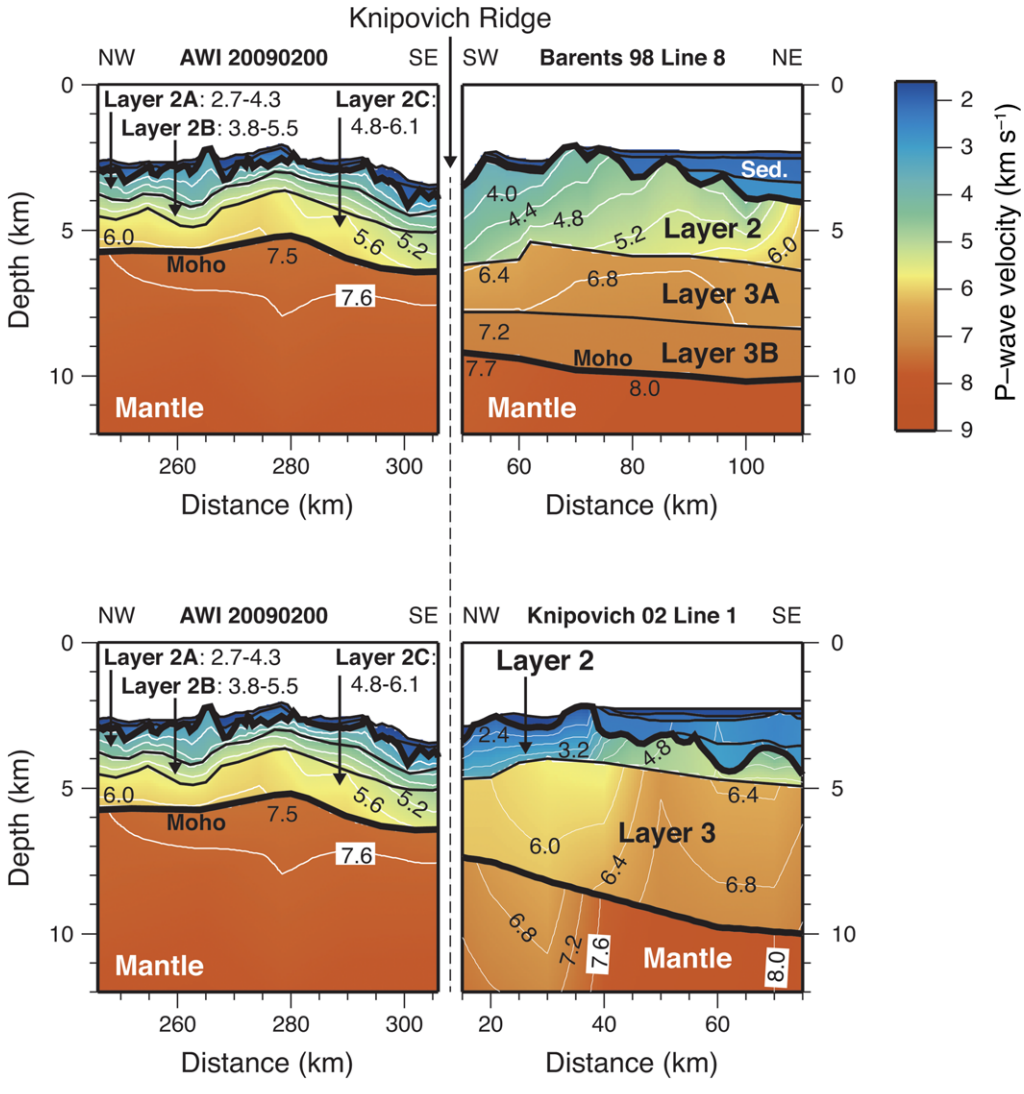

Fig. 10. Comparison of the P-wave velocity model of seismic refraction line AWI 20090200 (Hermann & Jokat 2013) with (top) the Barents 98 line 8 (Ljones *et al.* 2004), and (bottom) the Knipovich 02 line 1 (Kandilarov *et al.* 2008). For all lines, a 60 km-wide portion adjacent to the Knipovich Ridge is shown. Velocities are specified in km s^{-1}. Sed., sediments.

layer 2C on the AWI profile (4.8–6.1 km s^{-1}) and as layer 3 on the Knipovich 02 line 1 (5.6–7.0 km s^{-1}). Hence, based on the modelled velocities, the different interpretations seem to be justified. However, as discussed earlier, there is also the possibility that part of the interpreted layer 2C on the AWI line could be highly serpentinized mantle.

The definition of the Moho along the Knipovich 02 line 1 seems to be based mainly on mantle refractions (Pn). Kandilarov *et al.* (2008) showed only one station that recorded a Moho reflection (PmP) and here the misfit is up to 200 ms. Close to the Knipovich Ridge, the Moho is difficult to model with Pn phases alone, as the model indicates only a small velocity increase across the Moho. With that, there is no distinct change in the phase velocity of the first arrivals between the crustal and mantle arrivals that would allow for an unequivocal phase interpretation. From the previous discussion, it can be seen that the differences in the crustal structure of the lines at the Knipovich Ridge may, in fact, be less than that indicated by the velocity models.

In order to decide whether the differences are real or not, the lines should be reanalysed together.

Conclusions

The maps of the basement and Moho depth are useful tools to use in the discussion of first-order crustal features in the NE Atlantic realm. Although the region is not evenly covered with seismic refraction data and receiver function analyses, there is an adequate coverage of the large-scale tectonic structures. Data used in this compilation were acquired over a timespan of more than 40 years, and are therefore very variable in the shot and receiver spacing, as well as in the modelling technique. In addition, our understanding of rifting processes at continental margins has considerably changed over this period, which, of course, is reflected in the conceptual models on which the interpretation of the velocity models are based. Nevertheless, the basement and Moho depth are generally fairly robust features of velocity models, with the exception of areas with thin crust. Here, the mantle rock can be partially serpentinized and display velocities as low as 4.8 km s^{-1} at a serpentinization rate of 100% (Christensen 2004), and, hence, may erroneously be interpreted as crustal rock. One important measure of quality control for the basement and Moho compilation was the fit at cross-points to check for internal consistency of the datasets. While this helped to eliminate some erroneous data from the compilation, the maps are only as good as the underlying velocity models.

Using seismic refraction data to map the basement depth has two advantages compared to seismic reflection data. One is that no time-to-depth conversion is necessary as the velocity models are developed in the depth domain. The other is that the basement is often better defined on seismic refraction data, in particular in areas with deep sedimentary basins or where basalts are interbedded with sedimentary rocks. Many seismic refraction lines benefit from coincident reflection data by incorporating detailed basement relief from there. The disadvantage is that the data coverage with seismic refraction lines is not nearly as good as that with reflection lines. However, using the kriging method with gravity as a constraint, a rather detailed basement map could be compiled from the seismic refraction data (Fig. 3). That way, even basement lows that are not covered by seismic data are imaged, such as the Ammassalik Basin off SE Greenland. The basin depths of these seismically unconstrained features may be erroneous, but at least allow a qualitative assessment and comparison with the conjugate margin to be made (Fig. 8).

Our results show that the continuous rift basins extending from the southern Rockall Trough to the Lofoten Basin carry on to the Danmarkshavn and Thetis basins of NE Greenland (Fig. 8). Similarly, the Hatton Basin off Ireland seems to continue along with the Ammassalik Basin in SE Greenland. These correlations are most prominent on the basement map (Figs 3 & 8), while details of the Moho geometry beneath the Greenlandic basins are not resolved. This is related to a lack of seismic refraction data in these regions. However, 3D gravity modelling based on the seismic constraints is able to show a continuity of these features on the crustal thickness and Moho maps (Haase *et al.*, this volume, in review).

The crustal thickness that is compiled from the basement and Moho maps can be used to calculate crustal stretching factors and first-order crustal strength profiles, which has done by Kimbell *et al.* (this volume, in press) for the NW European margin. In addition, deformable plate reconstructions depend on good estimates of crustal thickness. Apparent inconsistencies in the crustal thickness map, such as the generally thinner oceanic crust west of the Knipovich Ridge compared to the east, can help to identify datasets that it might be worthwhile remodelling/reanalysing.

This work was part of the NAG-TEC project and was sponsored by BayernGas Norge AS, BP Exploration Operating Company Limited, Bundesanstalt für Geowissenschaften und Rohstoffe (BGR), Chevron East Greenland Exploration A/S, ConocoPhillips Skandinavia AS, DEA Norge AS, Det norske oljeselskap ASA, DONG E&P A/S, E.ON Norge AS, ExxonMobil Exploration and Production Norway AS, Japan Oil, Gas, and Metals National Corporation (JOGMEC), Maersk Oil, Nalcor Energy – Oil and Gas Inc., Nexen Energy ULC, Norwegian Energy Company ASA (Noreco), Repsol Exploration Norge AS, Statoil (U.K.) Limited, and Wintershall Holding GmbH. Reviews from Rolf Mjelde and an anonymous referee helped improve the manuscript. The work of Kenneth McDermott was supported by the Geological Survey of Ireland. Geoffrey S. Kimbell publishes with permission of the Executive Director of the British Geological Survey (Natural Environment Research Council).

References

Amante, C. & Eakins, B.W. 2009. *ETOPO1 1 Arc-Minute Global Relief Model: procedures, Data Sources and Analysis*. NOAA Technical Memorandum NESDIS NGDC-24 National Geophysical Data Center, NOAA, Washington, DC, https://doi.org/10.7289/V5C8276M

Andersen, O.B., Knudsen, P. & Berry, P.A.M. 2010. The DNSC08GRA global marine gravity field from double retracked satellite altimetry. *Journal of Geodesy*, **84**, 191–199, https://doi.org/10.1007/s00190-009-0355-9

Angenheister, G., Bjornsson, S. *et al.* 1980. Reykjanes Ridge Iceland Seismic Experiment (RRISP 77). *Journal of Geophysics*, **47**, 228–238.

Artemieva, I.M. & Thybo, H. 2013. EUNAseis: a seismic model for Moho and crustal structure in Europe, Greenland, and the North Atlantic region. *Tectonophysics*, **609**, 97–153, https://doi.org/10.1016/j.tecto.2013.08.004

Bamford, D., Nunn, K., Prodehl, C. & Jacob, B. 1977. LISPB–III. Upper crustal structure of northern Britain. *Journal of the Geological Society, London*, **133**, 481–488, https://doi.org/10.1144/gsjgs.133.5.0481

Bamford, D., Nunn, K., Prodehl, C. & Jacob, B. 1978. LISPB – IV. Crustal structure of Northern Britain. *Geophysical Journal of the Royal Astronomical Society*, **54**, 43–60, https://doi.org/10.1111/j.1365-246X.1978.tb06755.x

Barton, P.J. 1992. LISPB revisited: a new look under the Caledonides of northern Britain. *Geophysical Journal International*, **110**, 371–391, https://doi.org/10.1111/j.1365-246X.1992.tb00881.x

Barton, A.J. & White, R.S. 1997. Crustal structure of Edoras Bank continental margin and mantle thermal anomalies beneath the North Atlantic. *Journal of Geophysical Research*, **102**, 3109–3129, https://doi.org/10.1029/96jb03387

Berndt, C., Mjelde, R., Planke, S., Shimamura, H. & Faleide, J.I. 2001. Controls on the tectono-magmatic evolution of a volcanic transform margin: the Vøring Transform Margin, NE Atlantic. *Marine Geophysical Research*, **22**, 133–152, https://doi.org/10.1023/a:1012089532282

Bjarnason, I.T., Menke, W., Flóvenz, Ó.G. & Caress, D. 1993. Tomographic image of the Mid-Atlantic plate boundary in southwestern Iceland. *Journal of Geophysical Research*, **98**, 6607–6622, https://doi.org/10.1029/92jb02412

Böhner, J. & Antonić, O. 2008. Land-surface parameters specific to topo-climatology. *In*: Hengl, T. & Reuter, H.I. (eds) *Geomorphometry: Concepts, Software, Applications*. Developments in Soil Science, **33**. Elsevier, Amsterdam, 195–226, https://doi.org/10.1016/S0166-2481(08)00008-1

Bohnhoff, M. & Makris, J. 2004. Crustal structure of the southeastern Iceland-Faeroe Ridge (IFR) from wide aperture seismic data. *Journal of Geodynamics*, **37**, 233–252, https://doi.org/10.1016/j.jog.2004.02.004

Brandsdóttir, B., Hooft, E.E.E., Mjelde, R. & Murai, Y. 2015. Origin and evolution of the Kolbeinsey Ridge and Iceland Plateau, N-Atlantic. *Geochemistry, Geophysics, Geosystems*, **16**, 612–634, https://doi.org/10.1002/2014gc005540

Breivik, A.J., Mjelde, R., Grogan, P., Shimamura, H., Murai, Y., Nishimura, Y. & Kuwano, A. 2002. A possible Caledonide arm through the Barents Sea imaged by OBS data. *Tectonophysics*, **355**, 67–97, https://doi.org/10.1016/S0040-1951(02)00135-X

Breivik, A.J., Mjelde, R., Grogan, P., Shimamura, H., Murai, Y. & Nishimura, Y. 2003. Crustal structure and transform margin development south of Svalbard based on ocean bottom seismometer data. *Tectonophysics*, **369**, 37–70, https://doi.org/10.1016/s0040-1951 (03)00131-8

Breivik, A.J., Mjelde, R., Grogan, P., Shimamura, H., Murai, Y. & Nishimura, Y. 2005. Caledonide development offshore–onshore Svalbard based on ocean bottom seismometer, conventional seismic, and potential field data. *Tectonophysics*, **401**, 79–117, https://doi.org/10.1016/j.tecto.2005.03.009

Breivik, A.J., Mjelde, R., Faleide, J.I. & Murai, Y. 2006. Rates of continental breakup magmatism and seafloor spreading in the Norway Basin-Iceland plume interaction. *Journal of Geophysical Research*, **111**, B07102, https://doi.org/10.1029/2005jb004004

Breivik, A.J., Faleide, J.I. & Mjelde, R. 2008. Neogene magmatism northeast of the Aegir and Kolbeinsey ridges, NE Atlantic: spreading ridge–mantle plume interaction? *Geochemistry, Geophysics, Geosystems*, **9**, Q02004, https://doi.org/10.1029/2007gc001750

Breivik, A.J., Faleide, J.I., Mjelde, R. & Flueh, E.R. 2009. Magma productivity and early seafloor spreading rate correlation on the northern Vøring Margin, Norway – constraints on mantle melting. *Tectonophysics*, **468**, 206–223, https://doi.org/10.1016/j.tecto.2008.09.020

Breivik, A.J., Mjelde, R., Raum, T., Faleide, J.I., Murai, Y. & Flueh, E.R. 2011. Crustal structure beneath the Trøndelag Platform and adjacent areas of the Mid-Norwegian margin, as derived from wide-angle seismic and potential field data. *Norwegian Journal of Geology*, **90**, 141–161.

Bullock, A.D. & Minshull, T.A. 2005. From continental extension to seafloor spreading: crustal structure of the Goban Spur rifted margin, southwest of the UK. *Geophysical Journal International*, **163**, 527–546, https://doi.org/10.1111/j.1365-246X.2005.02726.x

Bunch, A.W.H. 1979. A detailed seismic structure of Rockall Bank (55°N, 15°W) – a synthetic seismogram analysis. *Earth and Planetary Science Letters*, **45**, 453–463, https://doi.org/10.1016/0012-821x(79)90144-4

Bunch, A.W.H. & Kennett, B.L.N. 1980. The crustal structure of the Reykjanes Ridge at 59° 30′N. *Geophysical Journal of the Royal Astronomical Society*, **61**, 141–166, https://doi.org/10.1111/j.1365-246X.1980.tb04310.x

Chabert, A., Ravaut, C., Readman, P.W., O'Reilly, B.M. & Shannon, P.M. 2006. Structure of the Hatton Basin (North Atlantic) from wide-angle and reflection seismic data. American Geophysical Union Fall Meeting, 11–15 December 2006, San Francisco, CA, USA. EOSTrans: AGU, 87 (52), Fall Meeting Supplement, Abstract T53A-1581.

Christensen, N.I. 2004. Serpentinites, peridotites, and seismology. *International Geology Review*, **46**, 795–816, https://doi.org/10.2747/0020-6814.46.9.795

Clark, S.A., Faleide, J.I. *et al.* 2013. Stochastic velocity inversion of seismic reflection/refraction traveltime data for rift structure of the southwest Barents Sea. *Tectonophysics*, **593**, 135–150, https://doi.org/10.1016/j.tecto.2013.02.033

Czuba, W., Ritzmann, O., Nishimura, Y., Grad, M., Mjelde, R., Guterch, A. & Jokat, W. 2004. Crustal structure of the continent–ocean transition zone along two deep seismic transects in north-western Spitsbergen. *Polish Polar Research*, **25**, 205–221.

Czuba, W., Ritzmann, O., Nishimura, Y., Grad, M., Mjelde, R., Guterch, A. & Jokat, W. 2005. Crustal structure of northern Spitsbergen along the deep seismic transect between the Molloy Deep and Nordaustlandet.

Geophysical Journal International, **161**, 347–364, https://doi.org/10.1111/j.1365-246X.2005.02593.x

Czuba, W., Grad, M. *et al.* 2008. Seismic crustal structure along the deep transect Horsted'05, Svalbard. *Polish Polar Research*, **29**, 279–290.

Czuba, W., Grad, M. *et al.* 2011. Continent–ocean-transition across a trans-tensional margin segment: off Bear Island, Barents Sea. *Geophysical Journal International*, **184**, 541–554, https://doi.org/10.1111/j.1365-246X.2010.04873.x

Dahl-Jensen, T., Thybo, H., Hopper, J. & Rosing, M. 1998. Crustal structure at the SE Greenland margin from wide-angle and normal incidence seismic data. *Tectonophysics*, **288**, 191–198, https://doi.org/10.1016/s0040-1951(97)00292-8

Dahl-Jensen, T., Larsen, T.B. *et al.* 2003. Depth to Moho in Greenland: receiver-function analysis suggests two Proterozoic blocks in Greenland. *Earth and Planetary Science Letters*, **205**, 379–393, https://doi.org/10.1016/s0012-821x(02)01080-4

Darbyshire, F.A., Bjarnason, I.T., White, R.S. & Flóvenz, Ó.G. 1998. Crustal structure above the Iceland mantle plume imaged by the ICEMELT refraction profile. *Geophysical Journal International*, **135**, 1131–1149, https://doi.org/10.1046/j.1365-246X.1998.00701.x

Darbyshire, F.A., White, R.S. & Priestley, K.F. 2000. Structure of the crust and uppermost mantle of Iceland from a combined seismic and gravity study. *Earth and Planetary Science Letters*, **181**, 409–428, https://doi.org/10.1016/s0012-821x(00)00206-5

DeMets, C., Gordon, R.G., Argus, D.F. & Stein, S. 1990. Current plate motions. *Geophysical Journal International*, **101**, 425–478, https://doi.org/10.1111/j.1365-246X.1990.tb06579.x

DeMets, C., Gordon, R.G., Argus, D.F. & Stein, S. 1994. Effect of recent revisions to the geomagnetic reversal time scale on estimates of current plate motions. *Geophysical Research Letters*, **21**, 2191–2194, https://doi.org/10.1029/94gl02118

Dick, H.J.B., Lin, J. & Schouten, H. 2003. An ultraslow-spreading class of ocean ridge. *Nature*, **426**, 405–412, https://doi.org/10.1038/nature02128

Digranes, P., Mjelde, R., Kodaira, S., Shimamura, H., Kanazawa, T., Shiobara, H. & Berg, E.W. 1998. A regional shear-wave velocity model in the central Vøring Basin, N. Norway, using three-component Ocean Bottom Seismographs. *Tectonophysics*, **293**, 157–174, https://doi.org/10.1016/s0040-1951(98)00093-6

Doré, A.G., Lundin, E.R., Jensen, L.N., Birkeland, Ø., Eliassen, P.E. & Fichler, C. 1999. Principal tectonic events in the evolution of the northwest European Atlantic margin. *In*: Fleet, A.J. & Boldy, S.A.R. (eds) *Petroleum Geology of Northwest Europe: Proceedings of the 5th Conference*. Geological Society, London, 41–61, https://doi.org/10.1144/0050041

Døssing, A. & Funck, T. 2012. Greenland Fracture Zone–East Greenland Ridge(s) revisited: indications of a C22-change in plate motion? *Journal of Geophysical Research*, **117**, B01103, https://doi.org/10.1029/2011jb008393

Døssing, A., Dahl-Jensen, T., Thybo, H., Mjelde, R. & Nishimura, Y. 2008. East Greenland Ridge in the North Atlantic Ocean: an integrated geophysical study of a continental sliver in a boundary transform fault setting. *Journal of Geophysical Research*, **113**, B10107, https://doi.org/10.1029/2007jb005536

Eccles, J.D., White, R.S., Robert, A.W., Christie, P.A.F. & the iSIMM Team 2007. Wide angle converted shear wave analysis of a North Atlantic volcanic rifted continental margin: constraint on sub-basalt lithology. *First Break*, **25**, 63–70, https://doi.org/10.3997/1365-2397.2007026

Eldholm, O. & Grue, K. 1994. North Atlantic volcanic margins: dimensions and production rates. *Journal of Geophysical Research*, **99**, 2955–2968, https://doi.org/10.1029/93jb02879

Erlendsson, Ö. & Blischke, A. 2013. *Law of the Sea. Seismic Reflection and Refraction Datasets. Status on the Processing and Interpretation Work*. Report. Iceland GeoSurvey (ÍSOR), Reykjavik.

Fliedner, M.M. & White, R.S. 2003. Depth imaging of basalt flows in the Faeroe–Shetland Basin. *Geophysical Journal International*, **152**, 353–371, https://doi.org/10.1046/j.1365-246X.2003.01833.x

Funck, T., Andersen, M.S., Keser Neish, J. & Dahl-Jensen, T. 2008. A refraction seismic transect from the Faroe Islands to the Hatton-Rockall Basin. *Journal of Geophysical Research*, **113**, B12405, https://doi.org/10.1029/2008jb005675

Funck, T., Andrup-Henriksen, G., Dehler, S.A. & Louden, K.E. 2012. The crustal structure of the Eirik Ridge at the southern Greenland continental margin. *In*: *Geological Association of Canada–Mineralogical Association of Canada Joint Annual Meeting*, St John's, Newfoundland & Labrador, 27–29 May 2012, Abstract Volume **35**, p. 47.

Funck, T., Hopper, J.R. *et al.* 2014. Crustal structure. *In*: Hopper, J.R., Funck, T., Stoker, M., Artling, U., Péron-Pindivic, G., Gaina, C. & Doornenbal, H. (eds) *NAG-TEC Atlas: Tectonostratigraphic Atlas of the North-East Atlantic Region*. Geological Survey of Denmark and Greenland (GEUS), Copenhagen, 69–126.

Funck, T., Gerlings, J. *et al.* 2015. The East Greenland Ridge: geophysical mapping and geological sampling reveal a highly segmented continental sliver. *In*: Smelror, M. (ed.) *7th International Conference on Arctic Margins – ICAM 2015*, Trondheim, Norway, 2–5 June 2015, NGU Report 2015.032. Geological Survey of Norway, Trondheim, p. 45.

Furmall, A.V. 2010. *Melt production and ridge geometry over the past 10 Myr on the southern Kolbeinsey Ridge, Iceland*. Master thesis, University of Oregon.

Gaina, C. 2014. Plate reconstructions and regional kinematics. *In*: Hopper, J.R., Funck, T., Stoker, M., Artling, U., Péron-Pindivic, G., Gaina, C. & Doornenbal, H. (eds) *NAG-TEC Atlas: Tectonostratigraphic Atlas of the North-East Atlantic Region*. Geological Survey of Denmark and Greenland (GEUS), Copenhagen, 53–66.

Gaina, C., Gernigon, L. & Ball, P. 2009. Palaeocene–Recent plate boundaries in the NE Atlantic and the formation of the Jan Mayen microcontinent. *Journal of the Geological Society, London*, **166**, 601–616, https://doi.org/10.1144/0016-76492008-112

Gebrande, H., Miller, H. & Einarsson, P. 1980. Seismic structure of Iceland along RRISP-profile I. *Journal of Geophysics*, **47**, 239–249.

Gerlings, J., Funck, T., Jackson, H.R., Louden, K.E. & Klingelhöfer, F. 2009. Seismic evidence for plume-derived volcanism during formation of the continental margin in southern Davis Strait and northern Labrador Sea. *Geophysical Journal International*, **176**, 980–994, https://doi.org/10.1111/j.1365-246X.2008.04021.x

Gerlings, J., Funck, T., Castro, C.F. & Hopper, J.R. 2014. The East Greenland Ridge – a continental sliver along the Greenland Fracture Zone. *Geophysical Research Abstracts*, **16**, EGU2014–EGU2879.

Gerlings, J., Hopper, J.R., Fyhn, M.B.W. & Frandsen, N.K. In review. Mesozoic rift basins on the SE Greenland shelf, near Ammassalik. *In*: Péron-Pinvidic, G., Hopper, J.R., Stoker, M.S., Gaina, C., Doornenbal, J.C., Funck, T. & Árting, U.E. (eds) *The NE Atlantic Region: A Reappraisal of Crustal Structure, Tectonostratigraphy and Magmatic Evolution*. Geological Society, London, Special Publications, **447**.

Goldflam, P., Weigel, W. & Loncarevic, B.D. 1980. Seismic structure along RRISP – profile 1 on the southeast flank of the Reykjanes Ridge. *Journal of Geophysics*, **47**, 250–260.

Grad, M., Tiira, T. & ESC Working Group 2009. The Moho depth map of the European Plate. *Geophysical Journal International*, **176**, 279–292, https://doi.org/10.1111/j.1365-246X.2008.03919.x

Gregersen, S., Clausen, C. & Dahl-Jensen, T. 1988. Crust and upper mantle structure in Greenland. *In*: *Proceedings of the 19th General Assembly of the European Seismological Commission*. Nauka, Moscow, 467–469.

Grevemeyer, I., Weigel, W., Dehghani, G.A., Whitmarsh, R.B. & Avedik, F. 1997. The Aegir Rift: crustal structure of an extinct spreading axis. *Marine Geophysical Research*, **19**, 1–23, https://doi.org/10.1023/a:1004288815129

Haase, C., Ebbing, J. & Funck, T. In review. A 3D regional custal model of the Northeast Atlantic based on seismic and gravity data. *In*: Péron-Pinvidic, G., Hopper, J.R., Stoker, M.S., Gaina, C., Doornenbal, J.C., Funck, T. & Árting, U.E. (eds) *The NE Atlantic Region: A Reappraisal of Crustal Structure, Tectonostratigraphy and Magmatic Evolution*. Geological Society, London, Special Publications, **447**.

Harland, K.E., White, R.S. & Soosalu, H. 2009. Crustal structure beneath the Faroe Islands from teleseismic receiver functions. *Geophysical Journal International*, **177**, 115–124, https://doi.org/10.1111/j.1365-246X.2008.04018.x

Hauser, F., O'Reilly, B.M., Jacob, A.W.B., Shannon, P.M., Makris, J. & Vogt, U. 1995. The crustal structure of the Rockall Trough: differential stretching without underplating. *Journal of Geophysical Research*, **100**, 4097–4116, https://doi.org/10.1029/94jb02879

Hauser, F., O'Reilly, B.M., Readman, P.W., Daly, J.S. & Van den Berg, R. 2008. Constraints on crustal structure and composition within a continental suture zone in the Irish Caledonides from shear wave wide-angle reflection data and lower crustal xenoliths. *Geophysical Journal International*, **175**, 1254–1272, https://doi.org/10.1111/j.1365-246X.2008.03945.x

Hermann, T. & Jokat, W. 2013. Crustal structures of the Boreas Basin and the Knipovich Ridge, North Atlantic. *Geophysical Journal International*, **193**, 1399–1414, https://doi.org/10.1093/gji/ggt048

Holbrook, W.S., Larsen, H.C. *et al.* 2001. Mantle thermal structure and active upwelling during continental breakup in the North Atlantic. *Earth and Planetary Science Letters*, **190**, 251–266, https://doi.org/10.1016/s0012-821x(01)00392-2

Hooft, E.E.E., Brandsdóttir, B., Mjelde, R., Shimamura, H. & Murai, Y. 2006. Asymmetric plume-ridge interaction around Iceland: the Kolbeinsey Ridge Iceland Seismic Experiment. *Geochemistry, Geophysics, Geosystems*, **7**, Q05015, https://doi.org/10.1029/2005gc001123

Hopper, J.R., Lizarralde, D. & Larsen, H.C. 1998. Seismic investigations offshore South-East Greenland. *Geology of Greenland Survey Bulletin*, **180**, 145–151.

Hopper, J.R., Dahl-Jensen, T. *et al.* 2003. Structure of the SE Greenland margin from seismic reflection and refraction data: implications for nascent spreading center subsidence and asymmetric crustal accretion during North Atlantic opening. *Journal of Geophysical Research*, **108**, 2269, https://doi.org/10.1029/2002jb001996

Hopper, J.R. *et al.* In prep. Sediment thickness and residual topography of the North Atlantic: estimating dynamic topography around Iceland. *In*: Péron-Pinvidic, G., Hopper, J.R., Stoker, M.S., Gaina, C., Doornenbal, J.C., Funck, T. & Árting, U.E. (eds) *The NE Atlantic Region: A Reappraisal of Crustal Structure, Tectonostratigraphy and Magmatic Evolution*. Geological Society, London, Special Publications, **447**.

Howell, S.M., Ito, G. *et al.* 2014. The origin of the asymmetry in the Iceland hotspot along the Mid-Atlantic Ridge from continental breakup to present-day. *Earth and Planetary Science Letters*, **392**, 143–153, https://doi.org/10.1016/j.epsl.2014.02.020

Hughes, S., Barton, P.J. & Harrison, D. 1998. Exploration in the Shetland-Faeroe Basin using densely spaced arrays of ocean-bottom seismometers. *Geophysics*, **63**, 490–501, https://doi.org/10.1190/1.1444350

Jacoby, W.R., Weigel, W. & Fedorova, T. 2007. Crustal structure of the Reykjanes Ridge near 62°N, on the basis of seismic refraction and gravity data. *Journal of Geodynamics*, **43**, 55–72, https://doi.org/10.1016/j.jog.2006.10.002

Jokat, W. 2010. *The Expedition of the Research Vessel 'Polarstern' to the Arctic in 2009 (ARK-XXIV/3)*. Reports on Polar and Marine Research, 615. Alfred Wegener Institute for Polar and Marine Research, Bremerhaven, Germany, https://doi.org/10013/epic.35320

Jokat, W., Ritzmann, O., Schmidt-Aursch, M.C., Drachev, S., Gauger, S. & Snow, J. 2003. Geophysical evidence for reduced melt production on the Arctic ultraslow Gakkel mid-ocean ridge. *Nature*, **423**, 962–965, https://doi.org/10.1038/nature01706

Jokat, W., Kollofrath, J., Geissler, W.H. & Jensen, L. 2012. Crustal thickness and earthquake distribution south of the Logachev Seamount, Knipovich Ridge.

Geophysical Research Letters, **39**, L08302, https://doi.org/10.1029/2012gl051199

Kaban, M.K., Flóvenz, Ó.G. & Pálmason, G. 2002. Nature of the crust-mantle transition zone and the thermal state of the upper mantle beneath Iceland from gravity modelling. *Geophysical Journal International*, **149**, 281–299, https://doi.org/10.1046/j.1365-246X.2002.01622.x

Kandilarov, A., Mjelde, R., Okino, K. & Murai, Y. 2008. Crustal structure of the ultra-slow spreading Knipovich Ridge, North Atlantic, along a presumed amagmatic portion of oceanic crustal formation. *Marine Geophysical Research*, **29**, 109–134, https://doi.org/10.1007/s11001-008-9050-0

Kandilarov, A., Landa, H., Mjelde, R., Pedersen, R., Okino, K. & Murai, Y. 2010. Crustal structure of the ultra-slow spreading Knipovich Ridge, North Atlantic, along a presumed ridge segment center. *Marine Geophysical Research*, **31**, 173–195, https://doi.org/10.1007/s11001-010-9095-8

Kandilarov, A., Mjelde, R. *et al.* 2012. The northern boundary of the Jan Mayen microcontinent, North Atlantic determined from ocean bottom seismic, multichannel seismic, and gravity data. *Marine Geophysical Research*, **33**, 55–76, https://doi.org/10.1007/s11001-012-9146-4

Kelly, A., England, R.W. & Maguire, P.K.H. 2007. A crustal seismic velocity model for the UK, Ireland and surrounding seas. *Geophysical Journal International*, **171**, 1172–1184, https://doi.org/10.1111/j.1365-246X.2007.03569.x

Kimbell, G.S., Ritchie, J.D., Johnson, H. & Gatliff, R.W. 2005. Controls on the structure and evolution of the NE Atlantic margin revealed by regional potential field imaging and 3D modelling. *In*: Doré, A.G. & Vining, B.A. (eds) *Petroleum Geology: North-West Europe and Global Perspectives – Proceedings of the 6th Petroleum Geology Conference*. Geological Society, London, 933–945, https://doi.org/10.1144/0060933

Kimbell, G.S., Stewart, M.A. *et al.* In press. Controls on the location of compressional deformation on the NW European margin. *In*: Péron-Pinvidic, G., Hopper, J.R., Stoker, M.S., Gaina, C., Doornenbal, J.C., Funck, T. & Árting, U.E. (eds) *The NE Atlantic Region: A Reappraisal of Crustal Structure, Tectonostratigraphy and Magmatic Evolution*. Geological Society, London, Special Publications, **447**, https://doi.org/10.1144/SP447.3

Klingelhöfer, F., Géli, L., Matias, L., Steinsland, N. & Mohr, J. 2000. Crustal structure of a super-slow spreading centre: a seismic refraction study of Mohns Ridge, 72°N. *Geophysical Journal International*, **141**, 509–526, https://doi.org/10.1046/j.1365-246x.2000.00098.x

Klingelhöfer, F., Edwards, R.A., Hobbs, R.W. & England, R.W. 2005. Crustal structure of the NE Rockall Trough from wide-angle seismic data modeling. *Journal of Geophysical Research*, **110**, B11105, https://doi.org/10.1029/2005jb003763

Kodaira, S., Mjelde, R., Gunnarsson, K., Shiobara, H. & Shimamura, H. 1997. Crustal structure of the Kolbeinsey Ridge, North Atlantic, obtained by use of ocean bottom seismographs. *Journal of Geophysical Research*, **102**, 3131–3151, https://doi.org/10.1029/96JB03487

Kodaira, S., Mjelde, R., Gunnarsson, K., Shiobara, H. & Shimamura, H. 1998*a*. Evolution of oceanic crust on the Kolbeinsey Ridge, north of Iceland, over the past 22 Myr. *Terra Nova*, **10**, 27–31, https://doi.org/10.1046/j.1365-3121.1998.00166.x

Kodaira, S., Mjelde, R., Gunnarsson, K., Shiobara, H. & Shimamura, H. 1998*b*. Structure of the Jan Mayen microcontinent and implications for its evolution. *Geophysical Journal International*, **132**, 383–400, https://doi.org/10.1046/j.1365-246x.1998.00444.x

Korenaga, J., Holbrook, W.S. *et al.* 2000. Crustal structure of the southeast Greenland margin from joint refraction and reflection seismic tomography. *Journal of Geophysical Research*, **105**, 21,591–21,614, https://doi.org/10.1029/2000JB900188

Kumar, P., Kind, R., Priestley, K. & Dahl-Jensen, T. 2007. Crustal structure of Iceland and Greenland from receiver function studies. *Journal of Geophysical Research*, **112**, B03301, https://doi.org/10.1029/2005jb003991

Kvarven, T., Ebbing, J. *et al.* 2014. Crustal structure across the Møre margin, mid-Norway, from wide-angle seismic and gravity data. *Tectonophysics*, **626**, 21–40, https://doi.org/10.1016/j.tecto.2014.03.021

Landes, M., Prodehl, C., Hauser, F., Jacob, A.W.B. & Vermeulen, N.J. 2000. VARNET-96: influence of the Variscan and Caledonian orogenies on crustal structure in SW Ireland. *Geophysical Journal International*, **140**, 660–676, https://doi.org/10.1046/j.1365-246X.2000.00035.x

Laske, G., Masters, G., Ma, Z. & Pasyanos, M. 2013. Update on CRUST1.0 – A 1-degree global model of Earth's crust. *Geophysical Research Abstracts*, **15**, EGU2013–EGU2658.

Libak, A., Eide, C.H., Mjelde, R., Keers, H. & Flüh, E.R. 2012*a*. From pull-apart basins to ultraslow spreading: results from the western Barents Sea Margin. *Tectonophysics*, **514–517**, 44–61, https://doi.org/10.1016/j.tecto.2011.09.020

Libak, A., Mjelde, R., Keers, H., Faleide, J.I. & Murai, Y. 2012*b*. An integrated geophysical study of Vestbakken Volcanic Province, western Barents Sea continental margin, and adjacent oceanic crust. *Marine Geophysical Research*, **33**, 185–207, https://doi.org/10.1007/s11001-012-9155-3

Licciardi, A., Piana Agostinetti, N., Lebedev, S., Schaeffer, A.J., Readman, P.W. & Horan, C. 2014. Moho depth and V_p/V_s in Ireland from teleseismic receiver functions analysis. *Geophysical Journal International*, **199**, 561–579, https://doi.org/10.1093/gji/ggu277

Ljones, F., Kuwano, A., Mjelde, R., Breivik, A., Shimamura, H., Murai, Y. & Nishimura, Y. 2004. Crustal transect from the North Atlantic Knipovich Ridge to the Svalbard Margin west of Hornsund. *Tectonophysics*, **378**, 17–41, https://doi.org/10.1016/j.tecto.2003.10.003

Lowe, C. & Jacob, A.W.B. 1989. A north-south seismic profile across the Caledonian Suture zone in Ireland. *Tectonophysics*, **168**, 297–318, https://doi.org/10.1016/0040-1951(89)90224-2

Mackenzie, G.D., Shannon, P.M., Jacob, A.W.B., Morewood, N.C., Makris, J., Gaye, M. & Egloff, F. 2002. The velocity structure of the sediments in the southern Rockall Basin: results from new wide-angle seismic modelling. *Marine and Petroleum Geology*, **19**, 989–1003, https://doi.org/10.1016/s0264-8172(02)00133-2

Makris, J., Egloff, R., Jacob, A.W.B., Mohr, P., Murphy, T. & Ryan, P. 1988. Continental crust under the southern Porcupine Seabight west of Ireland. *Earth and Planetary Science Letters*, **89**, 387–397, https://doi.org/10.1016/0012-821X(88)90 125-2

Makris, J., Ginzburg, A., Shannon, P.M., Jacob, A.W.B., Bean, C.J. & Vogt, U. 1991. A new look at the Rockall region, offshore Ireland. *Marine and Petroleum Geology*, **8**, 410–416, https://doi.org/10.1016/0264-8172(91)90063-7

Makris, J., Papoulia, I. & Ziska, H. 2009. Crustal structure of the Shetland–Faeroe Basin from long offset seismic data. *In*: *Faroe Islands Exploration Conference: Proceedings of the 2nd Conference*. *Annales Societatis Scientiarum Færoensis, Supplementum*, **50**, 30–42.

Mandler, H.A.F. & Jokat, W. 1998. The crustal structure of Central East Greenland: results from combined land–sea seismic refraction experiments. *Geophysical Journal International*, **135**, 63–76, https://doi.org/10.1046/j.1365-246X.1998.00586.x

Masson, F., Jacob, A.W.B., Prodehl, C., Readman, P.W., Shannon, P.M., Schulze, A. & Enderle, U. 1998. A wide-angle seismic traverse through the Variscan of southwest Ireland. *Geophysical Journal International*, **134**, 689–705, https://doi.org/10.1046/j.1365-246x.1998.00572.x

Menke, W., West, M., Brandsdóttir, B. & Sparks, D. 1998. Compressional and shear velocity structure of the lithosphere in northern Iceland. *Bulletin of the Seismological Society of America*, **88**, 1561–1571.

Minshull, T.A., Muller, M.R. & White, R.S. 2006. Crustal structure of the Southwest Indian Ridge at 66°E: seismic constraints. *Geophysical Journal International*, **166**, 135–147, https://doi.org/10.1111/j.1365-246X.2006.03001.x

Mjelde, R. 1992. Shear waves from three-component ocean bottom seismographs off Lofoten, Norway, indicative of anisotropy in the lower crust. *Geophysical Journal International*, **110**, 283–296, https://doi.org/10.1111/j.1365-246X.1992.tb00874.x

Mjelde, R. & Sellevoll, M.A. 1993. Seismic anisotropy inferred from wide-angle reflections off Lofoten, Norway, indicative of shear-aligned minerals in the upper mantle. *Tectonophysics*, **222**, 21–32, https://doi.org/10.1016/0040-1951(93)90187-O

Mjelde, R., Sellevoll, M.A., Shimamura, H., Iwasaki, T. & Kanazawa, T. 1992. A crustal study off Lofoten, N. Norway, by use of 3-component ocean bottom seismographs. *Tectonophysics*, **212**, 269–288, https://doi.org/10.1016/0040-1951(92)90295-H

Mjelde, R., Sellevoll, M.A., Shimamura, H., Iwasaki, T. & Kanazawa, T. 1993. Crustal structure beneath Lofoten, N. Norway, from vertical incidence and wide-angle seismic data. *Geophysical Journal International*, **114**, 116–126, https://doi.org/10.1111/j.1365-246X.1993.tb01471.x

Mjelde, R., Sellevoll, M.A., Shimamura, H., Iwasaki, T. & Kanazawa, T. 1995. S-wave anisotropy off Lofoten, Norway, indicative of fluids in the lower continental crust? *Geophysical Journal International*, **120**, 87–96, https://doi.org/10.1111/j.1365-246X.1995.tb05912.x

Mjelde, R., Kodaira, S. *et al.* 1997*a*. Comparison between a regional and semi-regional crustal OBS model in the Vøring Basin, Mid-Norway Margin. *Pure and Applied Geophysics*, **149**, 641–665, https://doi.org/10.1007/s000240050045

Mjelde, R., Kodaira, S., Shimamura, H., Kanazawa, T., Shiobara, H., Berg, E.W. & Riise, O. 1997*b*. Crustal structure of the central part of the Vøring Basin, mid-Norway margin, from ocean bottom seismographs. *Tectonophysics*, **277**, 235–257, https://doi.org/10.1016/S0040-1951(97)00028-0

Mjelde, R., Digranes, P. *et al.* 1998. Crustal structure of the northern part of the Vøring Basin, mid-Norway margin, from wide-angle seismic and gravity data. *Tectonophysics*, **293**, 175–205, https://doi.org/10.1016/s0040-1951(98)00090-0

Mjelde, R., Digranes, P. *et al.* 2001. Crustal structure of the outer Vøring Plateau, offshore Norway, from ocean bottom seismic and gravity data. *Journal of Geophysical Research*, **106**, 6769–6791, https://doi.org/10.1029/2000jb900415

Mjelde, R., Aurvåg, R., Kodaira, S., Shimamura, H., Gunnarsson, K., Nakanishi, A. & Shiobara, H. 2002*a*. V_p/V_s-ratios from the central Kolbeinsey Ridge to the Jan Mayen Basin, North Atlantic; implications for lithology, porosity and present-day stress field. *Marine Geophysical Research*, **23**, 123–145, https://doi.org/10.1023/a:1022439707307

Mjelde, R., Breivik, A.J. *et al.* 2002*b*. Geological development of the Sørvestsnaget Basin, SW Barents Sea, from ocean bottom seismic, surface seismic and potential field data. *Norwegian Journal of Geology*, **82**, 183–202.

Mjelde, R., Raum, T., Digranes, P., Shimamura, H., Shiobara, H. & Kodaira, S. 2003. V_p/V_s ratio along the Vøring Margin, NE Atlantic, derived from OBS data: implications on lithology and stress field. *Tectonophysics*, **369**, 175–197, https://doi.org/10.1016/s0040-1951(03)00198-7

Mjelde, R., Raum, T. *et al.* 2005. Continent-ocean transition on the Vøring Plateau, NE Atlantic, derived from densely sampled ocean bottom seismometer data. *Journal of Geophysical Research*, **110**, B05101, https://doi.org/10.1029/2004jb003026

Mjelde, R., Raum, T., Murai, Y. & Takanami, T. 2007. Continent–ocean-transitions: review, and a new tectono-magmatic model of the Vøring Plateau, NE Atlantic. *Journal of Geodynamics*, **43**, 374–392, https://doi.org/10.1016/j.jog.2006.09.013

Mjelde, R., Raum, T., Breivik, A. & Faleide, J. 2008. Crustal transect across the North Atlantic. *Marine Geophysical Research*, **29**, 73–87, https://doi.org/10.1007/s11001-008-9046-9

Mjelde, R., Raum, T., Kandilarov, A., Murai, Y. & Takanami, T. 2009. Crustal structure and evolution of the outer Møre Margin, NE Atlantic. *Tectonophysics*, **468**, 224–243, https://doi.org/10.1016/j.tecto.2008.06.003

Molinari, I. & Morelli, A. 2011. EPcrust: a reference crustal model for the European Plate. *Geophysical*

Journal International, **185**, 352–364, https://doi.org/10.1111/j.1365-246X.2011.04940.x

Mooney, W.D. & Brocher, T.M. 1987. Coincident seismic reflection/refraction studies of the continental lithosphere: a global review. *Reviews of Geophysics*, **25**, 723–742, https://doi.org/10.1029/RG025i004p00723

Morewood, N.C., Shannon, P.M. & Mackenzie, G.D. 2004. Seismic stratigraphy of the southern Rockall Basin: a comparison between wide-angle seismic and normal incidence reflection data. *Marine and Petroleum Geology*, **21**, 1149–1163, https://doi.org/10.1016/j.marpetgeo.2004.07.006

Morewood, N.C., Mackenzie, G.D., Shannon, P.M., O'Reilly, B.M., Readman, P.W. & Makris, J. 2005. The crustal structure and regional development of the Irish Atlantic margin region. *In*: Doré, A.G. & Vining, B.A. (eds) *Petroleum Geology: North-West Europe and Global Perspectives – Proceedings of the 6th Petroleum Geology Conference*. Geological Society, London, 1023–1033, https://doi.org/10.1144/0061023

Morgan, R.P.L., Barton, P.J., Warner, M., Morgan, J., Price, C. & Jones, K. 2000. Lithospheric structure north of Scotland – I. P-wave modelling, deep reflection profiles and gravity. *Geophysical Journal International*, **142**, 716–736, https://doi.org/10.1046/j.1365-246x.2000.00151.x

Navin, D.A., Peirce, C. & Sinha, M.C. 1998. The RAMESSES experiment – II. Evidence for accumulated melt beneath a slow spreading ridge from wide-angle refraction and multichannel reflection seismic profiles. *Geophysical Journal International*, **135**, 746–772, https://doi.org/10.1046/j.1365-246X.1998.00709.x

Olaya, V. & Conrad, O. 2008. Geomorphometry in SAGA. *In*: Hengl, T. & Reuter, H.I. (eds) *Geomorphometry: Concepts, Software, Applications*. Developments in Soil Science, **33**. Elsevier, Amsterdam, 293–308, https://doi.org/10.1016/S0166-2481(08)00012-3

O'Reilly, B.M., Shannon, P.M. & Vogt, U. 1991. Seismic studies in the North Celtic Sea Basin: implications for basin development. *Journal of the Geological Society, London*, **148**, 191–195, https://doi.org/10.1144/gsjgs.148.1.0191

O'Reilly, B.M., Hauser, F., Jacob, A.W.B. & Shannon, P.M. 1996. The lithosphere below the Rockall Trough: wide-angle seismic evidence for extensive serpentinisation. *Tectonophysics*, **255**, 1–23, https://doi.org/10.1016/0040-1951(95)00149-2

O'Reilly, B.M., Hauser, F. & Readman, P.W. 2010. The fine-scale structure of upper continental lithosphere from seismic waveform methods: insights into Phanerozoic crustal formation processes. *Geophysical Journal International*, **180**, 101–124, https://doi.org/10.1111/j.1365-246X.2009.04420.x

Parkin, C.J. & White, R.S. 2008. Influence of the Iceland mantle plume on oceanic crust generation in the North Atlantic. *Geophysical Journal International*, **173**, 168–188, https://doi.org/10.1111/j.1365-246X.2007.03689.x

Peron-Pinvidic, G., Gernigon, L., Gaina, C. & Ball, P. 2012. Insights from the Jan Mayen system in the Norwegian–Greenland sea – I. Mapping of a microcontinent. *Geophysical Journal International*, **191**, 385–412, https://doi.org/10.1111/j.1365-246X.2012.05639.x

Powell, C.M.R. & Sinha, M.C. 1987. The PUMA experiment west of Lewis, U.K. *Geophysical Journal of the Royal Astronomical Society*, **89**, 259–264, https://doi.org/10.1111/j.1365-246X.1987.tb04417.x

Price, C. & Morgan, J. 2000. Lithospheric structure north of Scotland – II. Poisson's ratios and waveform modelling. *Geophysical Journal International*, **142**, 737–754, https://doi.org/10.1046/j.1365-246x.2000.00204.x

Raum, T. 2000. *Crustal structure and evolution of the Faeroe, Møre and Vøring margins from wide-angle seismic and gravity data*. PhD thesis, University of Bergen, Norway.

Raum, T., Mjelde, R. *et al.* 2002. Crustal structure of the southern part of the Vøring Basin, mid-Norway margin, from wide-angle seismic and gravity data. *Tectonophysics*, **355**, 99–126, https://doi.org/10.1016/S0040-1951(02)00136-1

Raum, T., Mjelde, R. *et al.* 2005. Sub-basalt structures east of the Faroe Islands revealed from wide-angle seismic and gravity data. *Petroleum Geoscience*, **11**, 291–308, https://doi.org/10.1144/1354-079304-627

Raum, T., Mjelde, R. *et al.* 2006. Crustal structure and evolution of the southern Vøring Basin and Vøring Transform Margin, NE Atlantic. *Tectonophysics*, **415**, 167–202, https://doi.org/10.1016/j.tecto.2005.12.008

Ravaut, C., Chabert, A. *et al.* 2005. Wide-angle seismic imaging of the west Hatton margin (North Atlantic): Results of the HADES experiment. *Geophysical Research Abstracts*, **7**, 05509.

Reiche, S., Reid, I. & Thybo, H. 2011. Crustal structure of the Greenland-Iceland Ridge inferred from wide-angle seismic data. *Geophysical Research Abstracts*, **13**, EGU2011–EG11623.

Richardson, K.R., Smallwood, J.R., White, R.S., Snyder, D.B. & Maguire, P.K.H. 1998. Crustal structure beneath the Faroe Islands and the Faroe–Iceland Ridge. *Tectonophysics*, **300**, 159–180, https://doi.org/10.1016/s0040-1951(98)00239-x

Richardson, K.R., White, R.S., England, R.W. & Fruehn, J. 1999. Crustal structure east of the Faroe Islands: mapping sub-basalt sediments using wide-angle seismic data. *Petroleum Geoscience*, **5**, 161–172, https://doi.org/10.1144/petgeo.5.2.161

Rickers, F., Fichtner, A. & Trampert, J. 2013. The Iceland–Jan Mayen plume system and its impact on mantle dynamics in the North Atlantic region: evidence from full-waveform inversion. *Earth and Planetary Science Letters*, **367**, 39–51, https://doi.org/10.1016/j.epsl.2013.02.022

Ritzmann, O. & Jokat, W. 2003. Crustal structure of northwestern Svalbard and the adjacent Yermak Plateau: evidence for Oligocene detachment tectonics and non-volcanic breakup. *Geophysical Journal International*, **152**, 139–159, https://doi.org/10.1046/j.1365-246X.2003.01836.x

Ritzmann, O., Jokat, W., Mjelde, R. & Shimamura, H. 2002. Crustal structure between the Knipovich Ridge and the Van Mijenfjorden (Svalbard). *Marine Geophysical Research*, **23**, 379–401, https://doi.org/10.1023/B:MARI.0000018168.89762.a4

RITZMANN, O., JOKAT, W., CZUBA, W., GUTERCH, A., MJELDE, R. & NISHIMURA, Y. 2004. A deep seismic transect from Hovgård Ridge to northwestern Svalbard across the continental-ocean transition: a sheared margin study. *Geophysical Journal International*, **157**, 683–702, https://doi.org/10.1111/j.1365-246X.2004.02204.x

RITZMANN, O., MAERCKLIN, N., FALEIDE, J.I., BUNGUM, H., MOONEY, W.D. & DETWEILER, S.T. 2007. A three-dimensional geophysical model of the crust in the Barents Sea region: model construction and basement characterization. *Geophysical Journal International*, **170**, 417–435, https://doi.org/10.1111/j.1365-246X.2007.03337.x

ROBERTS, A.W., WHITE, R.S. & CHRISTIE, P.A.F. 2009. Imaging igneous rocks on the North Atlantic rifted continental margin. *Geophysical Journal International*, **179**, 1024–1038, https://doi.org/10.1111/j.1365-246X.2009.04306.x

ROBERTS, D.G., GINZBERG, A., NUNN, K. & MCQUILLIN, R. 1988. The structure of the Rockall Trough from seismic refraction and wide-angle reflection measurements. *Nature*, **332**, 632–635, https://doi.org/10.1038/332632a0

ROUZO, S., KLINGELHÖFER, F. *ET AL.* 2006. 2-D and 3-D modelling of wide-angle seismic data: an example from the Vøring volcanic passive margin. *Marine Geophysical Research*, **27**, 181–199, https://doi.org/10.1007/s11001-006-0001-3

SCHIFFER, C., BALLING, N., JACOBSEN, B.H., STEPHENSON, R.A. & NIELSEN, S.B. 2014. Seismological evidence for a fossil subduction zone in the East Greenland Caledonides. *Geology*, **42**, 311–314, https://doi.org/10.1130/G35244.1

SCHILLING, J.G., KINGSLEY, R., FONTIGNIE, D., POREDA, R. & XUE, S. 1999. Dispersion of the Jan Mayen and Iceland mantle plumes in the Arctic: a He-Pb-Nd-Sr isotope tracer study of basalts from the Kolbeinsey, Mohns, and Knipovich Ridges. *Journal of Geophysical Research*, **104**, 10,543–10,569, https://doi.org/10.1029/1999jb900057

SCHLINDWEIN, V. 2006. On the use of teleseismic receiver functions for studying the crustal structure of Iceland. *Geophysical Journal International*, **164**, 551–568, https://doi.org/10.1111/j.1365-246X.2006.02861.x

SCHLINDWEIN, V. & JOKAT, W. 1999. Structure and evolution of the continental crust of northern east Greenland from integrated geophysical studies. *Journal of Geophysical Research*, **104**, 15,227–15,245, https://doi.org/10.1029/1999JB900101

SCHMIDT-AURSCH, M.C. & JOKAT, W. 2005. The crustal structure of central East Greenland – I: from the Caledonian orogen to the Tertiary igneous province. *Geophysical Journal International*, **160**, 736–752, https://doi.org/10.1111/j.1365-246X.2005.02515.x

SCRUTTON, R.A. 1970. Results of a seismic refraction experiment on Rockall Bank. *Nature*, **227**, 826–827, https://doi.org/10.1038/227826a0

SCRUTTON, R.A. 1972. The crustal structure of Rockall Plateau microcontinent. *Geophysical Journal of the Royal Astronomical Society*, **27**, 259–275, https://doi.org/10.1111/j.1365-246X.1972.tb06092.x

SEDOV, V.V. & MAKRIS, J. 2001. Structure of the Earth's crust of the Iceland-Faeroe Ridge. *Oceanology*, **41**, 900–906.

SHANNON, P.M., JACOB, A.W.B., O'REILLY, B.M., HAUSER, F., READMAN, P.W. & MAKRIS, J. 1999. Structural setting, geological development and basin modelling in the Rockall Trough. *In*: FLEET, A.J. & BOLDY, S.A.R. (eds) *Petroleum Geology of Northwest Europe: Proceedings of the 5th Conference*. Geological Society, London, 421–431, https://doi.org/10.1144/0050421

SINHA, M.C., CONSTABLE, S.C. *ET AL.* 1998. Magmatic processes at slow spreading ridges: implications of the RAMESSES experiment at 57° 45′ N on the Mid-Atlantic Ridge. *Geophysical Journal International*, **135**, 731–745, https://doi.org/10.1046/j.1365-246X.1998.00704.x

SMALLWOOD, J.R. & WHITE, R.S. 1998. Crustal accretion at the Reykjanes Ridge, 61–62°N. *Journal of Geophysical Research*, **103**, 5185–5201, https://doi.org/10.1029/97jb03387

SMALLWOOD, J.R., WHITE, R.S. & MINSHULL, T.A. 1995. Sea-floor spreading in the presence of the Iceland plume: the structure of the Reykjanes Ridge at 61°40′N. *Journal of the Geological Society, London*, **152**, 1023–1029, https://doi.org/10.1144/GSL.JGS.1995.152.01.24

SMALLWOOD, J.R., TOWNS, M.J. & WHITE, R.S. 2001. The structure of the Faeroe-Shetland Trough from integrated deep seismic and potential field modelling. *Journal of the Geological Society, London*, **158**, 409–412, https://doi.org/10.1144/jgs.158.3.409

SMITH, L.K., WHITE, R.S., KUSZNIR, N.J. & ISIMM TEAM. 2005. Structure of the Hatton Basin and adjacent continental margin. *In*: DORÉ, A.G. & VINING, B.A. (eds) *Petroleum Geology: North-West Europe and Global Perspectives – Proceedings of the 6th Petroleum Geology Conference*. Geological Society, London, 947–956, https://doi.org/10.1144/0060947

SRIVASTAVA, S.P. & TAPSCOTT, C.R. 1986. Plate kinematics of the North Atlantic. *In*: VOGT, P.R. & TUCHOLKE, B.E. (eds) *The Geology of North America, Volume M, The Western North Atlantic Region*. Geological Society of America, Boulder, CO, 379–404.

STAPLES, R.K., WHITE, R.S., BRANDSDÓTTIR, B., MENKE, W., MAGUIRE, P.K.H. & MCBRIDE, J.H. 1997. Färoe-Iceland Ridge Experiment 1. Crustal structure of northeastern Iceland. *Journal of Geophysical Research*, **102**, 7849–7866, https://doi.org/10.1029/96jb03911

STEIN, M.L. 1999. *Interpolation of Spatial Data – Some Theory for Kriging*. Springer Series in Statistics. Springer, New York, https://doi.org/10.1007/978-1-4612-1494-6

STOREY, M., DUNCAN, R.A. & SWISHER, C.C. 2007. Paleocene-Eocene thermal maximum and the opening of the Northeast Atlantic. *Science*, **316**, 587–589, https://doi.org/10.1126/science.1135274

TOMLINSON, J.P., DENTON, P., MAGUIRE, P.K.H. & BOOTH, D.C. 2006. Analysis of the crustal velocity structure of the British Isles using teleseismic receiver functions. *Geophysical Journal International*, **167**,

223–237, https://doi.org/10.1111/j.1365-246X.2006.03044.x

VOGT, U., MAKRIS, J., O'REILLY, B.M., HAUSER, F., READMAN, P.W., JACOB, A.W.B. & SHANNON, P.M. 1998. The Hatton Basin and continental margin: crustal structure from wide-angle seismic and gravity data. *Journal of Geophysical Research*, **103**, 12,545–12,566, https://doi.org/10.1029/98jb00604

VOSS, M. & JOKAT, W. 2007. Continent–ocean transition and voluminous magmatic underplating derived from P-wave velocity modelling of the East Greenland continental margin. *Geophysical Journal International*, **170**, 580–604, https://doi.org/10.1111/j.1365-246X.2007.03438.x

VOSS, M. & JOKAT, W. 2009. From Devonian extensional collapse to early Eocene continental break-up: an extended transect of the Kejser Franz Joseph Fjord of the East Greenland margin. *Geophysical Journal International*, **177**, 743–754, https://doi.org/10.1111/j.1365-246X.2008.04076.x

VOSS, M., SCHMIDT-AURSCH, M.C. & JOKAT, W. 2009. Variations in magmatic processes along the East Greenland volcanic margin. *Geophysical Journal International*, **177**, 755–782, https://doi.org/10.1111/j.1365-246X.2009.04077.x

WARNER, M., MORGAN, J., BARTON, P., MORGAN, P., PRICE, C. & JONES, K. 1996. Seismic reflections from the mantle represent relict subduction zones within the continental lithosphere. *Geology*, **24**, 39–42, https://doi.org/10.1130/0091-7613(1996)024<0039:SRFTMR>2.3.CO;2

WEIGEL, W., FLÜH, E.R. *ET AL.* 1995. Investigations of the East Greenland continental margin between 70° and 72° N by deep seismic sounding and gravity studies. *Marine Geophysical Research*, **17**, 167–199, https://doi.org/10.1007/bf01203425

WEIR, N.R.W., WHITE, R.S., BRANDSDÓTTIR, B., EINARSSON, P., SHIMAMURA, H. & SHIOBARA, H. 2001. Crustal structure of the northern Reykjanes Ridge and Reykjanes Peninsula, southwest Iceland. *Journal of Geophysical Research*, **106**, 6347–6368, https://doi.org/10.1029/2000jb900358

WESSEL, P., SMITH, W.H.F., SCHARROO, R., LUIS, J. & WOBBE, F. 2013. Generic mapping tools: improved version released. *Eos, Transactions of the American Geophysical Union*, **94**, 409–410, https://doi.org/10.1002/2013eo450001

WHITE, R.S. 1997. Rift–plume interaction in the North Atlantic. *Philosophical Transactions of the Royal Society of London, Series A*, **355**, 319–339, https://doi.org/10.1098/rsta.1997.0011

WHITE, R.S. & MCKENZIE, D. 1995. Mantle plumes and flood basalts. *Journal of Geophysical Research*, **100**, 17,543–17,585, https://doi.org/10.1029/ 95jb01585

WHITE, R.S. & SMITH, L.K. 2009. Crustal structure of the Hatton and the conjugate east Greenland rifted volcanic continental margins, NE Atlantic. *Journal of Geophysical Research*, **114**, B02305, https://doi.org/10.1029/2008jb005856

WHITE, R.S., MCKENZIE, D. & O'NIONS, R.K. 1992. Oceanic crustal thickness from seismic measurements and rare earth element inversions. *Journal of Geophysical Research*, **97**, 19,683–19,715, https://doi.org/10.1029/92jb01749

WHITE, R.S., MINSHULL, T.A. *ET AL.* 1996. Seismic images of crust beneath Iceland contribute to long-standing debate. *Eos, Transactions of the American Geophysical Union*, **77**, 197–201, https://doi.org/10.1029/96eo00134

WHITE, R.S., FRUEHN, J., RICHARDSON, K.R., CULLEN, E., KIRK, W., SMALLWOOD, J.R. & LATKIEWICZ, C. 1999. Faeroes Large Aperture Research Experiment (FLARE): imaging through basalt. *In*: FLEET, A.J. & BOLDY, S.A.R. (eds) *Petroleum Geology of Northwest Europe: Proceedings of the 5th Conference*. Geological Society, London, 1243–1252, https://doi.org/10.1144/0051243

ZIEGLER, P. (ed.) 1988. *Evolution of the Arctic–North Atlantic and the Western Thetys*. American Association of Petroleum Geologists, Memoirs, **43**.